# Masses of Exotic Nuclei

Klaus Blaum, Sergey Eliseev, and Stephane Goriely

## Contents

### Abstract

Masses of exotic nuclei play a key role in multiple physics applications ranging from nuclear structure studies and input to astrophysical modeling to tests of the electroweak standard model, quantum electrodynamics, and neutrino physics. The nowadays most prominent mass spectrometry techniques rely on the storage and cooling of charged particles in multi-reflection time-of-flight, Penning-trap, and storage ring devices and the measurement of the revolution frequency of the ion of interest to a reference ion. We provide a comprehensive overview of these measurement techniques as well as the status of the most important

K. Blaum (✉) · S. Eliseev
MPI for Nuclear Physics, Heidelberg, Germany
e-mail: klaus.blaum@mpi-hd.mpg.de; sergey.eliseev@mpi-hd.mpg.de

S. Goriely
Institut d'Astronomie et d'Astrophysique, CP-226, Université Libre de Bruxelles, Brussels, Belgium
e-mail: Stephane.Goriely@ulb.be

1

mass measurements on exotic nuclei and their applications in atomic and nuclear physics.

We also review the various global mass models of interest for practical applications with a special emphasis on the two main widely developed approaches, i.e., the phenomenological macroscopic-microscopic and the semi-microscopic mean-field models. Both approaches can reach a root-mean-square deviation with respect to all the 2457 known masses better than typically 0.8 MeV. Such models need also to be tested with respect to their capacity to describe not only masses but also bulk structure properties like deformations, radii, as well as infinite nuclear-matter properties. While extrapolations by macroscopic-microscopic formulas remain unstable to different parametrization and to the incoherent link between the macroscopic part and the microscopic correction, mean-field models mainly suffer from uncertainties related to the type of adopted energy-density functional and the still large range of acceptable parameters. The different approaches typically lead to extrapolations toward experimentally unknown nuclei that can deviate by more than ∼5 MeV but also give rise to non-negligible variations of the pairing and shell effects.

## Introduction: Importance of Nuclear Masses for Nuclear Physics

More than 100 years after the first measurement of the charge/mass ratio of positive ions in discharge tubes (Thompson 1913), the study of atomic masses remains a field of active research, both experimentally and theoretically. Since then, it is clear that the mass $M(N, Z)$ of a nucleus with $N$ neutrons and $Z$ protons is measurably less than the sum of the masses of its constituent free nucleons. This opened extensive perspective to measure the binding energy of the nucleus and from it to study the many physical phenomena ruling the interactions of nucleons through the strong and Coulomb forces within the nucleus.

A century ago, Eddington (1920) understood that, through the mass defect, the nuclear transmutation of hydrogen into helium could be the main source of stellar energy and explain the long time scales of our sun. The intimate relationship between atomic mass measurements and astrophysics goes back to the earliest days of the field. Today, atomic masses are an essential ingredient of all models of stellar evolution and pervade all chapters of nuclear astrophysics (Arnould and Goriely 2020). The Universe is pervaded with nuclear physics imprints at all scales and atomic masses, and more particularly mass differences between the various species are the key ingredients dictating the various nuclear processes affecting both the energy produced or released and the change in the composition. The yellow squares in Fig. 1 illustrate the 2550 nuclei for which masses have been measured and evaluated in the latest Atomic Mass Evaluation (AME) of 2020 (Wang et al. 2021). Among them, 286 are naturally occurring, the remaining ones being artificially produced. The worldwide efforts devoted to mass measurements are reviewed in, e.g., Lunney et al. (2003), Blaum et al. (2013), Dilling et al. (2018), Lunney (2019), and below. This figure also shows the neutron and proton driplines. In the absence of
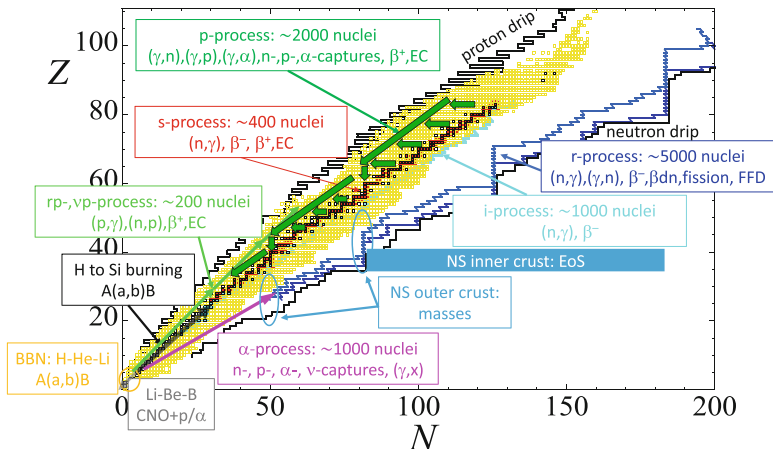
**Fig. 1** Schematic representation in the $(N, Z)$ plane of the different astronuclear physics applications, including nucleosynthesis processes and composition and structure properties of neutron stars. For each process, the nuclear needs are sketched. The open black squares correspond to stable or long-lived nuclei; the yellow squares to the nuclei for which masses have been measured and are included in the 2020 AME (Wang et al. 2021). Nuclei with neutron or proton separation energies tending to zero define the neutron or proton "driplines" (solid black lines), as predicted from a mass model. (More details can be found in Arnould and Goriely 2020)

complete experimental information, the driplines are essentially model dependent and are defined such that all nuclides lying between these lines are stable with respect to nucleon emission (although they become increasingly beta-unstable as the driplines are approached) and thus susceptible in principle to a measurement of their mass. It will be seen from Fig. 1 that while there are relatively few gaps on the proton-rich side, experimentalists already having reached the proton dripline at many places, there is a considerable lack of data on the neutron-rich side, especially at high mass numbers $A = N + Z$.

Figure 1 also illustrates the various nuclear data needs for stellar structure, stellar evolution, and nucleosynthesis applications (Arnould and Goriely 2020). The modeling of nucleosynthesis is certainly the most demanding regarding nuclear data, some processes requesting the consideration of as many as thousands of nuclides linked by a huge amount of nuclear reactions.

Most of the stellar evolution and nucleosynthesis processes can take full advantage of the high-precision mass measurements that have been performed for the last century (see below). These processes include the big-bang nucleosynthesis, the production of Li-Be-B by galactic cosmic rays (in particular CNO elements interacting with protons and $\alpha$-particles), hydrostatic and explosive burning stages of stellar evolution, the rapid proton-capture or $\nu$p processes in X-ray bursts or exploding massive stars, as well as the different nucleosynthesis processes responsible for the production of elements heavier than iron, such as the slow neutron-capture process (or s-process), the intermediate neutron-capture process (or

i-process), and the p-process. However, the lack of mass data on highly neutron-rich nuclei seriously limits our ability to understand the so-called rapid neutron-capture process (or r-process) of nucleosynthesis, the crust composition of neutron stars, and the cores of gravitationally collapsing stars. Despite the remarkable efforts of experimentalists in pushing ever closer to the neutron dripline, there is unfortunately no prospect of measuring the masses of many of the astrophysically relevant nuclei in the foreseeable future. For further progress one has to turn to theory.

## Experimental Aspects

### Modern Mass Spectrometry Techniques for Radionuclides

There is no general answer to the question of how precisely one has to determine masses of nuclides. The required uncertainty in mass determination is specific to the considered research subject. It has to be substantially smaller than the size of the investigated effect and thus can span many orders of magnitude.

For instance, in chemistry accurate mass measurements are used to identify elemental formulas of chemical compounds. The better the accuracy the less the ambiguity in this identification. Whereas for light molecules fractional uncertainties of $10^{-5}$ are sufficient to identify their composition, an unambiguous analysis of the composition of large molecules requires fractional uncertainties of about $10^{-6}$.

In nuclear physics required uncertainties range from approximately $10^{-6}$ down to $10^{-8}$ or so. Such mass measurements with seemingly moderate uncertainties are in reality very challenging, since the nuclides of interest are predominantly very short-lived with half-lives as short as a millisecond and even shorter. For instance, studies of the shell structure of nuclides as well as the investigation of the effects of nucleon-nucleon pairing are least demanding to precise mass measurements. Since the size of the nuclear shell gaps and the energy of the nucleon-nucleon pairing is on the order of a few MeV, fractional uncertainties of $10^{-6}$ in the measurements of the masses of the corresponding nuclides are totally sufficient. In halo nuclei the separation energies of loosely bound neutrons do not exceed a few hundred keV. Thus, the studies of the halo nuclei require mass measurements with uncertainties below $10^{-6}$. Substantially lower uncertainties of approximately $10^{-7}$ are needed in the search for low-lying nuclear isomeric states with excitation energies of a few 10 keV. Also the development of nuclear mass formulas benefits significantly from mass measurements with similar uncertainties.

Probably the lowest uncertainties of approximately $10^{-8}$ in the mass determination of short-lived nuclides are demanded in investigations of such properties of weak interaction as the unitarity of Cabibbo-Kobayashi-Maskawa (CKM) matrix and the test of the hypothesis of the conserved vector current (CVC).

Keeping in mind such a broad range of required uncertainties for mass measurements on nuclides that live a fraction of millisecond to some minutes, it is no surprise that there is no single "magic" mass-measurement technique that would be considered optimal for the entire ranges of the required mass-measurement

uncertainties and nuclide half-lives. All modern high-precision mass spectrometers that are employed in nuclear physics experiments fall into three classes: heavy-ion storage rings (Steck and Litvinov 2020), Penning traps, and multi-reflection time-of-flight (MR-ToF) devices. All these mass spectrometers are based on a common basic principle – a "storage" of nuclides in ionic states for a sufficiently long time in a combination of stable static electric and magnetic fields. The storage of ions results in a dramatic increase of their flight path, the attainable resolving power, and hence the precision in the determination of their masses. The strength of mass spectrometers based on heavy-ion storage rings is their ability to measure masses of nuclides with extremely short-lived half-lives of a fraction of a millisecond. Another unique feature of such mass spectrometers is its ability to perform simultaneous mass measurements on a broad spectrum of nuclides with various mass-to-charge ratios. The MR-ToF mass spectrometers unlike storage rings are very compact, table-size devices that allow for mass measurements with uncertainties down to $10^{-7}$ on single nuclides that live just a few 10 milliseconds. As soon as nuclides with half-lives of a fraction of a second and longer are addressed and mass-measurement uncertainties of $10^{-8}$ are considered, Penning-trap mass spectrometers are the only choice.

### Heavy-Ion Storage Rings

There are three operating heavy-ion storage rings in the world. These are the experimental storage ring (ESR) at the GSI Helmholtzzentrum für Schwerionenforschung in Germany (Franzke 1987), the experimental cooler storage ring (CSRe) at the Institute of Modern Physics (IMP) in China (Xia et al. 2002), and the rare-RI ring (R3) at the RI Beam Factory (RIBF) of RIKEN in Japan (Ozawa et al. 2012).

Such heavy-ion storage rings are huge machines with a typical circumference of a few ten to a hundred meters and the beam energy of a few to a few hundred MeV (Fig. 2). Their design is governed by the corresponding accelerator facilities that define the primary ion beam and its energy. The primary beam impinges on a thin target which is placed between the accelerator and the storage ring. The fast reaction products after in-flight separation are injected into the storage ring. Since the in-flight separation of fast ions is a rapid process, reaction products with half-lives well below a millisecond can be stored and addressed in the storage ring.

The revolution frequency spread $\Delta f/f$ of the ions in the storage ring is governed by (Geissel et al. 1992)

$$\frac{\Delta f}{f} = -\frac{1}{\gamma_t^2}\frac{\Delta(m/q)}{(m/q)} + (1 - \frac{\gamma^2}{\gamma_t^2})\frac{\Delta v}{v}, \tag{1}$$

where $\Delta v/v$ is the velocity spread of the ions, $\gamma$ is the relativistic Lorentz factor, $\gamma_t^2$ is the transition point of the ring, and $m$ and $q$ are the mass and the charge of the ions, respectively. The revolution frequency of an ion is proportional to its mass-to-charge ratio if the second term of equation 1 can be made negligible. This can be reached either by reducing the velocity spread of the reaction products in the ring or
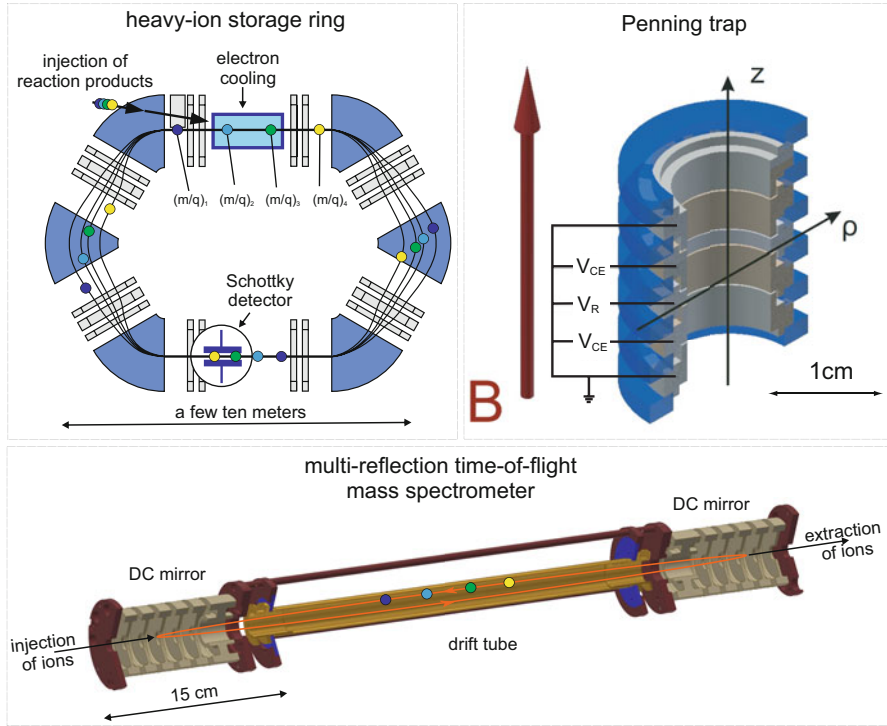
**Fig. 2** Schematic illustration of three ion storage devices: (1) a heavy-ion storage ring by the example of the ESR storage ring in the Schottky mode, (2) a five-pole cylindrical Penning trap, and (3) a multi-reflection time-of-flight mass spectrometer

by operating the storage ring at transition ($\gamma = \gamma_t$). The former underlies Schottky mass spectrometry (SMS) (Franzke et al. 2008) and is achieved by employing the stochastic and/or electron cooling techniques (Steck et al. 2004; Nolden et al. 2004). The latter builds a basis for isochronous mass spectrometry (IMS) (Franzke et al. 2008). Since cooling takes a few seconds, the SMS technique is applied to relatively long-lived nuclides. The frequencies of the cooled reaction products are measured nondestructively with a Schottky noise detector. In the IMS no cooling of the reaction products is required. This makes the IMS technique suitable for mass measurements on very short-lived nuclides with half-lives even shorter than a millisecond. The revolution times of the reaction products are measured with dedicated time-of-flight microchannel plate detectors.

Both techniques were developed at the ESR at the GSI Helmholtzzentrum für Schwerionenforschung. First mass measurements on proton-rich isotopes in the range of $60 \leq Z \leq 84$ with the SMS technique date back to 1997 (Radon et al. 1997), and the ESR remains the only storage ring where the SMS technique in its classical form is employed. Mass-measurement programs at the other two storage rings are conducted exclusively with the IMS technique. The need to use electron

cooling in the SMS technique sets a severe constraint to the half-lives accessible with this technique. As a result, only a few broadband SMS measurements were carried out, and thus further application of the SMS is limited. Thus, the future of mass measurements in storage rings is associated with the development of the IMS technique. The first pilot mass-measurement experiment with the IMS technique took place at the ESR in 2004 (Stadlmann et al. 2004). Masses of some isotopes of V, Mn, Ti, and Cr with half-lives down to 50 ms were determined with uncertainties of 100 to 500 keV/c$^2$. Since the IMS technique does not require cooling of reaction products, it is presently the fastest mass-measurement method which is based on ion storage. The mass measurement on a 4.6 MeV isomer in $^{133}$Sb with the IMS technique is the mass measurement on the shortest-lived nuclide ($T_{1/2} = 17\,\mu s$) ever measured with mass spectrometry techniques (Sun et al. 2010).

The future of mass spectrometry in storage rings is solely related to further developments of the IMS technique. Two very promising developments are currently undertaken at CSRe in China. One is the implementation of two time-of-flight detectors in the ring in order to measure the velocities of ions in addition to the revolution times (Shuai et al. 2016). This allows one to reduce the negative influence of the velocity spread on the performance of the IMS technique and thus to substantially increase the mass resolving power of the technique. The other development to improve the performance of the IMS technique is a replacement of the time-of-flight microchannel plate detector with a nondestructive Schottky noise detector (Tu et al. 2018).

### Multi-reflection Time-of-Flight Mass Spectrometers

Mass spectrometry in heavy-ion storage rings is a fast developing branch of mass-measurement techniques due to its ability to perform broadband mass measurements on very short-lived nuclides. Nevertheless, this technique has a severe "drawback." Heavy-ion storage rings are huge costly machines that demand for their development large manpower, technical, and material resources. Thus, each such a machine is in fact unique and is part of a large accelerator facility. The idea of having a tabletop mass spectrometer that can in some aspects compete with the SMS/IMS techniques and can be employed for mass measurements at even moderate-size rare-ion-beam (RIB) setups is very attractive. One of such techniques is time-of-flight mass spectrometry (ToF-MS). The concept of ToF-MS was first presented by W.E. Stephen in 1946 and implemented in 1948 by A.E. Cameron and D.F. Eggers (Cameron and Eggers 1948). In spite of a constant development of the technique, until 1990 it did not raise any interest in the field of mass measurements on rare nuclides, because the ToF mass spectrometers were single-pass devices with a very moderate resolving power. The turning point in the field of ToF-MS in nuclear physics came in 1990, when the concept of multi-reflection time-of-flight mass spectrometry (MR-ToF-MS) was introduced (Wollnik and Przewloka 1990).

If ions pass the spectrometer's flight path back and forth many times until they acquire a sufficiently long time of flight, it can result in a high mass resolving power. To provide such a multi-pass regime, a short bunch of ions is injected between two axially symmetric coaxial electrostatic mirrors that reflect the trapped ions back and

forth until the ions get injected toward a detector for time-of-flight measurements (Fig. 2). A typical MR-ToF mass spectrometer employed for mass measurements on rare nuclides is about a meter long and has a kinetic energy of trapped ions of approximately 1 kV and a bunch length of a few hundred ns. The mass spectrometer is operated in the isochronous mode for a certain ion kinetic-energy range. This provides a linear increase of the mass resolving power with the time of flight in the ToF range up to a few 10 milliseconds. Further increase of the time of flight leads to a leveling off the resolving power at a value of a few hundred thousand. This is caused by an instability of the mirrors' electric potentials, a residual gas pressure, and various imperfections of the ion optical elements. Thus, the niche of MR-ToF mass spectrometers are presently mass measurements with fractional uncertainties down to approximately $10^{-7}$ on nuclides with half-lives as short as a few milliseconds. The MR-ToF devices can operate as mass spectrometers and as mass separators in two regimes: (1) in a broad mass-band regime with a low mass resolving power and (2) in a narrow mass-band regime with a high mass resolving power. Potentially, MR-ToF mass spectrometers are capable of measuring with a moderate uncertainty masses of very short-lived nuclides with half-lives shorter than a millisecond. In practice, the cooling, pre-separation, and preparation of ions prior to their injection into the MR-ToF mass spectrometer take at least several milliseconds and hence set a low limit on the half-lives of nuclides whose masses can be measured with a MR-ToF mass spectrometer.

Although the basic operation principles of MR-ToF-MS were introduced in 1990, it took 23 years until such a MR-ToF mass spectrometer was employed at the ISOLTRAP facility at ISOLDE/CERN in an online experiment for separating $^{82}$Zn ions of interest from by far more abundant contaminant $^{82}$Rb ions (Wolf et al. 2013). A short time after that, two groups reported almost simultaneously on the first online measurements on short-lived nuclides. The group at ISOLTRAP conducted a mass measurement on $^{51}$Ca and $^{52}$Ca isotopes, whereas the SLOWRI team from RIKEN measured the mass of $^{8}$Li (Ito et al. 2013).

Today, such MR-ToF mass spectrometers are in operation or under construction at many RIB facilities: ISOLTRAP (Wolf et al. 2013), SLOWRI at RIBF/RIKEN (Ito et al. 2013), RISP at RAON (Daejeon, South Korea) (Yoon et al. 2014), TITAN at ISAC/TRIUMF (Vancouver, Canada) (Jesch et al. 2015), the FRS Ion-Catcher at FRS/GSI (Darmstadt, Germany) (Dickel et al. 2015), PILGRIM at S3-SPIRAL2/GANIL (Caen, France) (Chauveau et al. 2016), CARIBU at ATLAS/ANL (Argonne, USA) (Hirsh et al. 2016), the Notre Dame Cyclotron Facility (Notre Dame, USA) (Schultz et al. 2016), SHANS at IMP/CAS (Lanzhou, China) (Wang et al. 2020), and MARA-LEB at the University of Jyväskylä (Jyväskylä, Finland) (Uusitalo et al. 2019). At a half of these facilities, they can operate not only as stand-alone mass spectrometers but also in conjunction with Penning traps as high-resolution mass separators.

## Penning Traps

As soon as masses of nuclides with half-lives longer than a few hundred milliseconds have to be determined with a fractional uncertainty smaller than $10^{-7}$, there

is only one choice – Penning-trap mass spectrometry (PTMS). The era of PTMS on rare nuclides began in 1987 (Bollen et al. 1987) with a measurement of the mass of $^{77,78,85,86,88}$Rb and $^{88}$Sr at the pioneering Penning-trap mass spectrometer ISOLTRAP (Kluge and Bollen 1993) that is situated at ISOLDE/CERN. For more than a decade, ISOLTRAP remained the only player in the field of PTMS on rare nuclides, until in 2000s new PTMS facilities began to operate one by one at various RIB facilities throughout the world (Dilling et al. 2000, 2003; Savard et al. 2001; Ringle et al. 2009; Eronen et al. 2012; Ketelaer et al. 2008).

The superiority of PTMS over the other two mass-measurement techniques is based on a very small ion storage volume of a fraction of just a cubic millimeter. In the Penning trap, ions are stored in a combination of a strong homogeneous static magnetic field of a few tesla and a weak quadrupole (harmonic) electrostatic potential. Such an electrostatic harmonic trapping potential can be created by two electrodes that are hyperboloids of revolution. In practice one tends to use a stack of five cylindrical electrodes (see Fig. 2) for this instead due to a much simpler manufacturing of such a structure. The trapped ion performs three trap motions – cyclotron, magnetron, and axial – with frequencies $\nu_+$, $\nu_-$, and $\nu_z$, respectively. The sum of the cyclotron and magnetron frequencies is used in PTMS on rare nuclides to determine the mass $m$ of the ion according to the following relations:

$$\frac{1}{2\pi}\frac{q}{m}B = \nu_c = \nu_+ + \nu_-, \tag{2}$$

where $q$ is the ion's charge, $B$ is the magnetic field strength, and $\nu_c$ is the free cyclotron frequency of the ion.

Today two techniques to measure the free cyclotron frequency are employed in PTMS on rare nuclides – (1) time-of-flight ion-cyclotron resonance (ToF-ICR) and (2) phase-imaging ion-cyclotron resonance (PI-ICR) techniques. The ToF-ICR technique was introduced in 1980 by Gräff et al. for a measurement of the proton-to-electron mass ratio. In 1987 it was for the first time applied at ISOLTRAP for mass measurements on rare nuclides (Bollen et al. 1987). Since then, the ToF-ICR technique has been subject to steady developments (Bollen et al. 1992; König et al. 1995; Kretzschmar 2007; George et al. 2007; Eliseev et al. 2007; Ringle et al. 2007) and until 2013 was the only cyclotron-frequency measurement technique used in PTMS on rare nuclide. It is based on the measurement of the time of flight of an ion between the trap that is placed in a strong magnetic field and a multichannel plate detector that is located on the axis of the trap in a region of weak magnetic field. The ion on its way toward the detector passes the region with a strong gradient of the magnetic field, where it gets accelerated. This force and hence the ion's time of flight depend on the orbital magnetic moment of the ion in the trap. By altering the ion's orbital magnetic moment by means of rf fields of certain multipolarity with certain frequency and amplitude, one obtains a ToF resonance (see Fig. 3). By fitting to the experimental points a corresponding theoretical function, one determines the free cyclotron frequency of the ion.
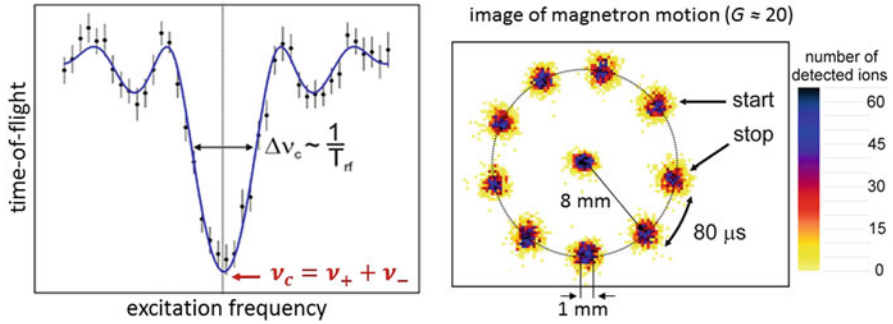
**Fig. 3** (left) A typical time-of-flight ion-cyclotron resonance. The blue curve is a theoretical function fit to the experimental data points (König et al. 1995). (right) A projection with a magnification $G = 20$ of the ion's magnetron motion at different ion trapping times onto a position-sensitive detector

In 2013 the PI-ICR technique was developed at the SHIPTRAP experiment (Eliseev et al. 2013, 2014) for the determination of the $Q$-values of the $\beta^-$ decay of $^{187}$Re and of the electron capture in $^{163}$Ho with a for online PTMS unprecedentedly low uncertainty of approximately 30 eV (Eliseev et al. 2015a; Nesterenko et al. 2014). The operation principle of this technique is absolutely different to that of the ToF-ICR technique. With the PI-ICR method, one measures the total phase $\phi$ a certain trap motion accumulates in a well-defined time $t$ and determines the corresponding frequency of this motion as

$$\nu = \frac{1}{2\pi} \frac{\phi + 2\pi n}{2\pi t}, \tag{3}$$

where $n$ is the number of full revolutions the ion performs in time $t$. The total phase is determined by projecting the ion position in the trap onto a position-sensitive detector (see Fig. 3). The PI-ICR technique offers compared to the ToF-ICR technique gains in precision and in resolving power of approximately 5 and 40, respectively. This makes possible to resolve nuclear isomeric states with excitation energies of just a few 10 keV and half-lives of a fraction of a second. Due to the demonstrated performance, the PI-ICR technique is becoming the mass-measurement technique of choice at more and more Penning-trap facilities, thus replacing the ToF-ICR technique (Manea et al. 2020; Lykiardopoulou et al. 2020; Nesterenko et al. 2018; Orford et al. 2020).

## Mass Spectrometry on Radioactive Ions

### Nuclear Structure Studies

A central and probably the most intriguing question of nuclear physics can be shaped into a short phrase: "Where does nuclear matter cease to exist?" A

combination of protons and neutrons is considered a nucleus if it lives longer than a typical time of strong interaction ($10^{-22}$ s). In practice however it is often impossible to measure such short life times of nuclei, and hence this definition of nuclear-matter existence is of little practical use. Instead, experimentalists have introduced an alternative criterion of the existence of nuclear matter which is based on the concept of the proton and neutron driplines (Thoennessen 2004). The stability of a nucleus with a certain number of protons and neutrons is determined by the separation energy required to remove a single proton (separation energy $S_p$) or a single neutron (separation energy $S_n$) from a nucleus. A general dependence of $S_p$ and $S_n$ on the number of protons and neutrons in nuclei is well described by the simple liquid-drop model of nucleus (Gamow 1930). The more (less) neutrons a nuclide with a certain $Z$ has, the smaller the $S_n$ ($S_p$) becomes. The lines that correspond to $S_p = 0$ and $S_n = 0$ are referred to as the proton and the neutron dripline, respectively. In order to determine the location of the driplines on the nuclear chart, it is necessary to calculate the separation energies from the masses of the corresponding nuclides using the following formulas:

$$
\begin{aligned}
S_p &= [M(Z-1, N) - M(Z, N) + m_p] \cdot c^2, \\
S_n &= [M(Z, N-1) - M(Z, N) + m_n] \cdot c^2,
\end{aligned}
\tag{4}
$$

where $m_p$ and $m_n$ are the masses of a proton and neutron, respectively, and $M(Z, N)$ is the mass of a nuclide with $Z$ protons and $N$ neutrons. Thus, measurements of the masses of nuclides in the vicinity of the driplines are of primary importance in order to establish the boundaries of the nuclear-matter existence. The realizability of such extremely challenging mass measurements almost solely relies on a development of different experimental techniques for a production of nuclides in the vicinity of the driplines. The proton dripline has experimentally been reached due to its relatively near location to the valley of $\beta$-stability for all odd-$Z$ elements from Li ($Z = 3$) to Np ($Z = 93$) (Zhang et al. 2019) and for a range of even-$Z$ elements (Blank and Płoszajczak 2008). The progress in the localizing the neutron dripline in contrast is very moderate – the neutron dripline has been traced only up to neon (Ahn et al. 2019). Unlike a proton, a neutron is electrically neutral, and hence nuclides with even very large excess of neutrons remain relatively long-lived. Thus, the neutron dripline in the medium and heavy mass regions is located many dozens neutron numbers away off the valley of $\beta$-stability and with high certainty will not be experimentally reached in the next several decades. Presently the only possibility to get a clue about an approximate location of the neutron dripline is the consideration of the trend of the neutron separation energies calculated for all nuclides with measured masses and the extrapolation of this trend to $S_n=0$ employing various mass formulas (Sobiczewski et al. 2018). In this approach high-precision mass measurements with a few 10 keV/c$^2$ uncertainty on all experimentally reachable nuclides become mandatory.

One- and two-nucleon separation energies are in general a very powerful tool in nuclear structure studies. Irregularities and discontinuities in their behavior reflect

various changes in the structure of corresponding nuclides, e.g., the closure of a nuclear shell (Caurier et al. 2005), the onset of a deformation (Bohr and Mottelson 1998), the presence of shape coexistence configurations (Wood et al. 1992), the appearance of a neutron halo (Jensen et al. 2004; Riisager 2013), etc. As an illustration to this, let us consider by selected examples the role of the two-neutron separation energies in the studies of the nuclear shell evolution and of light neutron-halo nuclei.

The shell model of a nucleus proposed and developed in the 1930s and 1940s of the past century states that nuclei with certain, magic, numbers of nucleons (2, 8, 20, 28, 50, 82, 126) are more tightly bound than the neighboring nuclei with higher numbers of nucleons. The effect can be quantified in the most convenient way with a proton $\Delta_p$ and neutron $\Delta_n$ shell gaps

$$
\begin{aligned}
\Delta_p(Z_m, N) &= S_{2p}(Z_m, N) - S_{2p}(Z_m + 2, N), \\
\Delta_n(Z, N_m) &= S_{2n}(Z, N_m) - S_{2n}(Z, N_m + 2),
\end{aligned}
\tag{5}
$$

where $Z_m$ and $N_m$ denote the proton and neutron magic number, respectively. A typical size of the shell gap amounts to a few MeV/c$^2$ for nuclei in the vicinity of the valley of $\beta$-stability. Nuclides with a very unbalanced ratio of neutron number to proton number, i.e., nuclides near the nucleon driplines, can substantially differ from the stable nuclides in their nuclear properties, in particular in the structure of the nuclear shells. For instance, the magic numbers can change, and the size of the shell gaps can alter. Even a complete disappearance of the shell structure is not excluded. The easiest way to study the evolution of the nuclear shell structure is measurements of masses of light nuclides. Just an addition of one nucleon to a light nucleus drastically alters the neutron-to-proton-number ratio resulting in this mass region in a very close location of the driplines to the valley of $\beta$-stability. A prominent example of such a study is precision mass measurements on the isotope sequences $^{29-31}$Ne and $^{30-34}$Mg (Chaudhuri et al. 2013). They have demonstrated the extinction of the $N = 20$ neutron shell closure for $^{32}$Mg.

Another spectacular finding in the region of light nuclides was the discovery of nuclei with unexpectedly large nuclear-matter radii – halo nuclei. The story began in 1985 with a measurement of the interaction cross section of $^{11}$Li in a fragmentation reaction of $^{20}$Ne on $^{12}$C (Tanihata et al. 1985). The calculated nuclear-matter radius of $^{11}$Li surprisingly turned out to be comparable to that of heavy $^{208}$Pb. Such swell of $^{11}$Li is caused by a large excess of neutrons over protons in the nucleus. This leads to a weak coupling of two last neutrons to the core nucleus $^9$Li and hence to a significant extension of their wavefunction to a larger radius. The most straightforward way to test the strength of the two-neutron coupling is a direct measurement of the two-neutron separation energy. It was performed in 2008 by directly measuring the mass difference of $^9$Li and $^{11}$Li (369.15(65) keV) with the Penning-trap mass spectrometer TITAN (Smith et al. 2008). Since then a dozen proton- and neutron-halo nuclei have been discovered with the heaviest being $^{22}$C (a two-neutron halo) and $^{27}$S (a two-proton halo), and a search for further ones is ongoing.

## Nuclear Astrophysics Studies

A precise knowledge of the masses of thousands of nuclides located between the proton and neutron drip lines (see Fig. 1) plays a key role in our understanding of the origin of the elements in the Universe, as explained in section "Introduction: Importance of Nuclear Masses for Nuclear Physics". Very light nuclides such as hydrogen, helium, and a certain amount of lithium were synthesized shortly after the Big Bang (Pitrou et al. 2018). These nuclides became seeds for the production of heavier nuclides up to iron in nuclear fusion reactions in stars over the course of millions to billions of years of their evolution (Arnould and Goriely 2020; Kobayashi et al. 2020). Since nuclides around iron are the most bound ones, nuclear synthesis by charged-particle reactions ceases in this region. Nuclides heavier than iron up to uranium are synthesized in neutron capture reactions (Arnould and Goriely 2020).

About a half of nuclides heavier than iron are produced predominantly via the slow neutron capture process (or $s$-process) in the C-rich layers of asymptotic-giant-branch (AGB) stars (Karakas 2010; Goriely and Siess 2018) as well as during core He-burning in massive stars (Choplin et al. 2018). In this process, stable seed nuclides inside a star can occasionally capture a neutron producing nuclides with a higher mass number. The process is called slow because the neutron flux in such stars is weak resulting in the time between two neutron captures of many years or even hundreds of years. If the new nuclide is unstable, it usually $\beta^-$ decays to a heavier element before it can capture a new neutron. This process repeats many times until it is terminated in the region around lead, bismuth, and polonium. Thus, the $s$-process proceeds along the valley of $\beta$ stability. The masses of nuclides along the $s$-process path are known already precisely enough, and the main nuclear physics input required to model the $s$-process are the neutron-capture reaction rates (see Fig. 1).

The other half of the nuclides in the valley of $\beta$ stability are mainly synthesized by the rapid neutron-capture process ($r$-process) (Arnould et al. 2007; Cowan et al. 2007). This process is entirely responsible for the production of the most neutron-rich isotopes of stable elements and all long-lived elements heavier than bismuth, including Th and U in particular. Many stable nuclides are produced by both the $s$- and $r$-processes. The $r$ process may potentially occur during core-collapse supernova explosions of massive stars (Janka 2017; Wanajo et al. 2018), in jet-like explosions of magnetorotational core-collapse supernovae (Nishimura et al. 2015; Reichert et al. 2021) and their collapsar remnant (Siegel et al. 2019) as well as in binary neutron star mergers (Goriely et al. 2011; Metzger et al. 2010; Just et al. 2015). In such environments, large neutron densities between $10^{24}$ and $10^{34}$ cm$^{-3}$ may eventually be found leading to a series of neutron captures on timescales of the order of $\mu$s and the production of exotic neutron-rich nuclei. Temperatures above 1 GK are usually found in such astrophysical plasma, so that photoneutron emission may slow down the nuclear flow toward the neutron drip line. On timescales of milliseconds, $\beta^-$ decay brings the flow toward heavier and heavier elements until it reaches the actinide region where fission may recycle material down to lighter mass fragments. During the neutron irradiation, the $r$-process proceeds close to

the neutron drip line along nuclides with a neutron separation energy between 0 and 3 MeV depending on the time evolution of the neutron density and temperature. When all free neutrons are captured, the exotic neutron-rich nuclei decay back to the valley of $\beta$ stability, mainly by $\beta^-$ decay but also for the heaviest nuclei by $\alpha$-decay and spontaneous fission. The $r$-process nuclear flow, hence the abundances of produced nuclides, strongly depends on the competition between neutron captures and photoneutron emission, hence on the neutron separation energies of nuclides, hence on their masses. The underlying exponential dependence between neutron captures and photoneutron emission requires the knowledge of the masses of the involved nuclides with an uncertainty better than typically 10 to $100 \, \text{keV/c}^2$ in order to provide an efficient constraint for mass formulas. Today one cannot experimentally produce the exotic neutron-rich nuclides produced during the $r$-process neutron irradiation and theory needs to fill the gaps (see section "Nuclear Mass Models and Theoretical Approaches"). Thus, currently it remains to perform high-precision mass measurements on the majority of experimentally accessible less neutron-rich nuclides. Such measurements provide extremely valuable input data for mass formulas employed to calculate the neutron separation energies for nuclides of $r$-process relevance (Canete et al. 2020; Vilen et al. 2018, 2020; Orford et al. 2018; Hartley et al. 2018; Van Schelt et al. 2012, 2013; Reiter et al. 2020; Klawitter et al. 2016; Atanasov et al. 2015).

The $s$ and $r$ processes account for a production of about 99% of nuclides observed in nature. The remaining 1% are stable neutron-deficient nuclides between selenium and mercury, the so-called $p$-nuclides (Arnould and Goriely 2003). In contrast to the $s$- and $r$-processes calling for neutron captures to explain the production of heavy elements, the $p$ isotopes are mainly produced by photodisintegration reactions on already-synthesized $s$ and $r$ nuclei. These photoreactions involve $(\gamma,n)$, $(\gamma,p)$, and $(\gamma,\alpha)$ reactions at stellar temperatures of the order of 2–3 $10^9$ K. The $p$ nuclides are mostly produced in the final explosion of a massive star ($M \gtrsim 10 \, M_\odot$) as a core-collapse supernova or in pre-explosive oxygen burning episodes (Arnould and Goriely 2003). The $p$ process can develop in the O-Ne layers of the massive stars explosively heated to peak temperatures ranging between 1.7 and 3.3 $10^9$ K (Rayet et al. 1995; Travaglio et al. 2018). The seeds for the $p$ process are provided by the $s$ process that develops before the explosion in these stellar mass zone. In this way, the O-Ne layers that experience the $p$ process are initially enriched in $70 \lesssim A \lesssim 90$ s-nuclides. Type Ia supernovae have also been suggested as a potential site for the $p$ process. The $p$-process nucleosynthesis possibly accompanying the deflagration or delayed detonation regimes has been mainly studied in one-dimensional simulations and shown to give rather similar overabundances as core-collapse supernovae models (Arnould and Goriely 2003; Travaglio et al. 2018). However, the predicted $p$ nuclide yields from type Ia supernovae suffer from large uncertainties affecting the adopted explosion models as well as the $s$-seed distributions, detailed information on the composition of the material that is pre-explosively transferred to the white dwarf being missing.

Another astrophysical site of particular interest for nuclear mass measurements concerns the rapid proton capture (or $rp$ process) taking place in a high-temperature

high-density proton-rich environment (Schatz et al. 1998; Parikh et al. 2013). This process is expected to happen during X-ray burst corresponding to a binary star system in which a neutron star accretes matter (predominantly hydrogen) on its surface from the companion star. A high density of the accreted matter results in a runaway thermonuclear explosion creating appropriate conditions for the $rp$ process to occur. The $rp$ process is, however, not followed by mass ejection due to the strong neutron star gravitational field, so that it is not expected to contribute to the Galactic enrichment in heavy elements (Parikh et al. 2013). The nuclear dynamics of the $rp$ process is relatively similar to that of the $r$ process but on the neutron-deficient side of the valley of $\beta$ stability. Seed nuclides successively capture protons until the proton drip line is reached. A further capture of a proton is inhibited by the reverse process of proton emission. This equilibrium holds until the involved nuclides at the proton drip line undergo $\beta^+$ decay producing proton-rich isotopes of a heavier element. This process of capturing protons with subsequent $\beta^+$ decay repeats many times until it is terminated by the $\alpha$-decay of tin, antimony, and tellurium isotopes. Thus, the $rp$ process runs along the proton drip line and its exact path depends on the thermodynamic conditions of the astrophysical plasma, but also on the masses of the nuclides produced close to the proton drip line. Unlike the neutron drip line, the proton drip line is located much closer to the valley of $\beta$ stability and thus the masses of the majority of $rp$ process-related nuclides have been already experimentally determined (Fallis et al. 2011; Chowdhury et al. 2015; Ong et al. 2018; Puentes et al. 2020; Valverde et al. 2018; Haettner et al. 2011). As an illustration of such a high-precision mass measurement with a large impact on the modeling of the $rp$ process let us consider the measurement with SHIPTRAP of the masses of proton-rich nuclides located in the nuclear chart between rubidium and technetium (Haettner et al. 2011). A determination with a few keV/c$^2$ uncertainties of the masses of ten nuclides produced in a fusion-evaporation reaction of a $^{36}$Ar beam on a $^{54}$Fe target yielded a systematic shift of the mass surface by up to 1.6 MeV/c$^2$ causing abundance changes of the ashes of astrophysical X-ray bursts.

**Fundamental Interactions and Standard Model Tests**

The highest precision in a determination of the masses of exotic nuclides is required for studies of fundamental interactions and tests of the standard model of particle physics (SM). By exotic nuclides we understand not only short-lived nuclides but also long-lived (sometimes almost stable) nuclides that can undergo exotic decay processes. In this subchapter we focus on three studies: (1) an investigation of weak interaction by testing the unitarity of Cabibbo-Kobayashi-Maskawa (CKM) matrix and the hypothesis of the conserved vector current (CVC) (Hardy and Towner 2020), (2) a search for neutrinoless double-beta processes (Avignone et al. 2008; Blaum et al. 2020), and (3) a determination of the neutrino mass (Formaggio et al. 2021).

In the SM the quark mass eigenstates (the quantum states of quarks when they propagate freely) differ from the quark weak eigenstates (the quantum states of quarks that participate in electroweak interactions). The transformation of one set of quark eigenstates into the other one is described by the quark-mixing matrix known as CKM matrix. In the SM this matrix is required to be unitary, i.e.,

$$|V_{ud}|^2 + |V_{us}|^2 + |V_{ub}|^2 = 1, \tag{6}$$

where $V_{ud}$, $V_{us}$, and $V_{ub}$ are the elements of the first row of the CKM matrix that are determined from weak decays of the corresponding quarks. Thus, a determination of nonunitarity of the CKM matrix will be a hint at the existence of new physics beyond the SM. Due to a pronounced difference in the values of the top row's elements ($V_{ud} \approx 0.97$, $V_{us} \approx 0.22$, and $V_{ub} < 0.004$), a determination of $V_{ud}$ is the most important. The $V_{ud}$ matrix element can be expressed through the weak-interaction coupling constant $G_F$ (determined from muon decay) and the vector coupling constant $G_v$ as $V_{ud} = G_v/G_F$. The vector coupling constant can be determined most precisely from an investigation of superallowed $\beta$-decay between nuclear states with $(J^\pi, T) = (0^+, 1)$. Such transitions depend uniquely on the vector part of the weak interaction. According to the CVC hypothesis, in the SM the vector part of the weak interaction is not influenced by the strong interaction, and hence the experimental "corrected" $Ft$-values for such transitions are directly related to the vector coupling constant, which is the same for all of them:

$$Ft = \frac{K}{2G_v^2(1 + \Delta_R^v)}. \tag{7}$$

$K$ and $\Delta_R^v$ are transition-independent corrections. The $Ft$-value depends on the $Q$-value of the considered transition, i.e., on the difference of the masses of the parent and daughter nuclides of the transition. Since the $Q$-value enters the $Ft$-value in the fifth order, it has to be determined very precisely, with fractional uncertainties of approximately $10^{-8}$. Twenty-three superallowed $\beta$-decay transitions are currently under scrutiny (the lightest decaying nuclide is $^{10}$C; the heaviest, $^{74}$Rb). The $Q$-values of 17 transitions from this group already have been determined directly with Penning traps with sufficiently low uncertainties of approximately $10^{-8}$ and better (see Table 1 in Hardy and Towner 2020 and the references therein). The other six are still waiting their turn. The first violin in these measurements was played by the Penning-trap mass spectrometer JYFLTRAP which accounts for the determination of the $Q$-values of 13 transitions.

Another prominent example of the search for new physics beyond the SM are experiments that struggle to observe neutrinoless double-beta transitions (Racah 1937; Furry 1939). In the "classical" SM, neutrinos and antineutrinos are different massless Dirac particles. Nevertheless, we already know from the discovery of neutrino oscillations that neutrinos do have mass (Fukuda et al. 1998). The massiveness of neutrinos renders feasible the realization of a second scenario – neutrinos and antineutrinos are identical, i.e., Majorana particles. The answer to the question whether neutrinos and antineutrinos are Dirac or Majorana particles can be found most conveniently from the investigation of neutrinoless double $\beta^-$ decay ($0\nu2\beta^-$ decay) (Avignone et al. 2008) and neutrinoless double-electron capture ($0\nu2EC$) (Blaum et al. 2020). These extremely rare neutrinoless double-beta processes with expected half-lives of substantially longer than $10^{25}$ years can

happen only if neutrinos are Majorana particles. One expects that $0\nu2\beta^-$ decay is in general a by far more probable process than $0\nu2EC$, and hence until now all efforts have been put in the search for $0\nu2\beta^-$ decay. There is a bunch of large-scale experiments that are devoted to this search (Barabash 2017). In these experiments one searches in the energy-sum spectrum of two emitted electrons for a signature of $0\nu2\beta^-$ decay – a peak at an energy that equals the $Q$-value of the process. This search is hampered by a continuous spectrum from by far more probable two-neutrino double $\beta^-$ decay. Thus, it is crucial to know the $Q$-values of all double $\beta^-$-decay transitions of interest with uncertainties of approximately 1 keV in order to be able to localize in the energy-sum spectrum the peak from $0\nu2\beta^-$ decay. Furthermore, a measurement of the $Q$-values along with the half-lives of $0\nu2\beta^-$-decay transitions will allow for the determination of the effective Majorana neutrino mass. Since the nuclides of interest that can undergo $0\nu2\beta^-$ decay are in fact stable and hence are available in a sufficiently large amount, all most prominent double $\beta^-$-decay transitions have already been addressed by various Penning-trap facilities, and their Q-values have already been determined with sufficiently low uncertainties (Table 2 in Dilling et al. 2018 and references therein).

$0\nu2EC$ with its expected half-life in general exceeding $10^{30}$ years is in practice a non-observable process, and as a result no single large-scale experiment has been established yet to search for this process. Nevertheless, in some rare cases, its probability can be increased by many orders of magnitude, i.e., resonantly enhanced, and becomes comparable to that of $0\nu2\beta^-$ decay. The probability of a $0\nu2EC$ transition is proportional to a resonant factor $F$

$$F = \frac{\Gamma_{2h}}{(Q - B_{2h} - E_\gamma)^2 + \Gamma_{2h}^2/4} = \frac{\Gamma_{2h}}{\Delta^2 + \Gamma_{2h}^2/4}, \tag{8}$$

where $\Gamma_{2h}$, $Q$, $B_{2h}$, $E_\gamma$, and $\Delta$ are the width of the final state of the transition, the $Q$-value of the transition, the binding energy of the two captured electrons, the energy of the nuclear excited state populated by this transition, and the degeneracy factor, respectively. One can talk about a substantial increase of a particular $0\nu2EC$ transition if its degeneracy factor does not exceed few hundred eV. Thus, a determination with an uncertainty of about 100 eV of the $Q$-values of promising $0\nu2EC$ transitions is essential in a search for a resonantly enhanced transition. An extensive experimental campaign has recently been undertaken for a search for such a resonantly enhanced transition. In this series of experiments, the $Q$-values of 19 double EC transitions have been determined at various Penning-trap facilities, predominantly at the facility SHIPTRAP (Tables 6 and 7 in Blaum et al. 2020 and references therein). Two $0\nu2EC$ transitions – $^{152}$Gd$\rightarrow^{152}$Sm (Eliseev et al. 2011b) and $^{156}$Dy$\rightarrow^{156}$Gd (Eliseev et al. 2011a) – turn out to be at least partially resonantly enhanced. The expected half-lives of these transitions normalized to the effective Majorana neutrino mass value of 1 eV exceed $10^{26}$ years/eV. This half-life is too long to begin a search for $0\nu2EC$. Thus, all efforts in the near future will still be focused solely on the search for $0\nu2\beta^-$ decay.

This subchapter is concluded with a brief description of the role of high-precision Penning-trap mass spectrometry in the determination of the neutrino mass. The only model-independent way to determine the electron neutrino mass is investigations of beta-processes ($\beta^-$ decay and electron capture (EC)). Two such processes are of particular interest – the $\beta^-$ decay of tritium and the electron capture in $^{163}$Ho – due to their exceptionally small $Q$-values and hence high sensitivity to the neutrino mass. Three experiments are presently in different phases of construction (Gastaldo et al. 2017; Alpert et al. 2015; Esfahani et al. 2017), and one already takes data (Aker et al. 2021) with the goal to push the upper limit on the neutrino mass well below 1 eV/c$^2$. The neutrino mass is determined from the analysis of the end-point region of either the emitted electron spectrum of tritium $\beta^-$ decay or the atomic de-excitation spectrum of the EC in $^{163}$Ho. The $Q$-values of these processes measured directly and independently with a fractional uncertainty $\delta Q/M$ well below $10^{-11}$ ($M$ is the mass of the nuclide of the corresponding process) will facilitate an assessment of the systematic uncertainty in the neutrino mass determination. The FSU trap has already approached this goal quite near for the $Q$-value of the tritium $\beta^-$ decay by measuring the mass difference of tritium and $^3$He with an uncertainty of 70 meV ($\delta Q/M \approx 2.3 \cdot 10^{-11}$) (Myers et al. 2015). Another Penning-trap mass spectrometer, namely, SHIPTRAP, has determined the $Q$-value of the EC in $^{163}$Ho with an uncertainty of approximately 33 eV ($\delta Q/M \approx 2 \cdot 10^{-10}$) (Eliseev et al. 2015b) having solved the long-standing problem with a substantial disagreement between the $Q$-values obtained with different techniques. Nevertheless, the achieved uncertainty is still large compared to about 1 eV required for the determination of the neutrino mass with a sub-eV/c$^2$ uncertainty. Such a precise determination of the $Q$-value of the EC in $^{163}$Ho is planned to be performed in the near future with the Penning-trap mass spectrometer PENTATRAP (Schüssler et al. 2020; Filianin et al. 2021).

## Nuclear Mass Models and Theoretical Approaches

Generally speaking, the more fundamental the theory used, the greater should be one's confidence in the prediction of nuclear masses. For this reason, one of the major goals of modern nuclear physics remains to derive masses, along with other nuclear properties, from the "real" basic interactions between nucleons, as determined by the measured properties of two- and three-nucleon systems (both scattering and bound states), with some guidance from meson theory and quantum chromodynamics. However, the resolution of the many-body problem remains extremely complicated, and it is only in the last few years that it has become possible to calculate ab initio nuclear masses with an accuracy approaching that required in applications and even then only in the case of the lightest $A \lesssim 80$ nuclei (see Tichai et al. 2020; Hergert 2020, for reviews). This approach has also been successful in estimating homogeneous or infinite nuclear matter (INM), a limiting case of ordinary nuclei with an infinite number of nucleons and with no Coulomb interactions. Although such a system is purely hypothetical, it is of great theoretical interest in that being the simplest many-body nuclear system, it serves as a test

bench for the various ab initio methods, but also as important constraints for nuclear mass models.

Since there is no chance to predict all nuclear masses of interest in nuclear applications (including in particular astrophysics) in a near future from ab initio methods, mass models have turned toward "semiempirical" approaches in the sense that the theoretical description of the nucleus that is adopted always consists of a model with a number of free parameters that are fitted to the measured masses (and potentially to other nuclear data). Thus theory is used simply as a means of extrapolating from the mass data to the unknown nuclides (and to INM). However, in addition to predicting masses of unmeasured nuclei, nuclear mass formulas also provide a wealth of information about static as well as dynamic nuclear properties, such as nuclear deformations, nuclear radii, single-particle level schemes, pairing strength, etc. These quantities are of particular relevance for the calculation of reaction cross sections or decay rates, and when not available experimentally, these quantities are traditionally extracted from a mass model which aims at reproducing *all* measured masses as accurately as possible, i.e., with a root-mean-square (rms) deviation smaller than typically 0.7–0.8 MeV. The importance of estimating all ground-state properties reliably should not be underestimated. For example, the nuclear level density of a deformed nucleus at low energies (typically at the neutron separation energy) is predicted to be significantly (about 30 to 50 times) larger than of a spherical one due principally to the rotational enhancement (Capote et al. 2009). An erroneous determination of a quantity like the nuclear deformation can therefore lead to large errors in the estimate of, e.g., radiative neutron-capture cross sections.

For specific applications such as nuclear astrophysics or accelerator-driven systems, a large number of data need to be extrapolated far away from the experimentally known region. In this case, two major features of the nuclear theory must be contemplated, namely, its *reliability* and *accuracy*. A microscopic description by a physically sound model based on first principles ensures a reliable extrapolation away from experimentally known region. For this reason, use is made preferentially of microscopic or semi-microscopic global predictions based on sound and reliable nuclear models which, in turn, can compete with more phenomenological highly parametrized models in the reproduction of experimental data. The selection criterion of the adopted model is fundamental, since the extrapolation in a domain out of reach of laboratory measurements by parametrized systematics based on experimental data can fail drastically. Global microscopic approaches have been developed for the last decades and are now more or less well understood. However, they are rarely used for practical applications, because of their lack of accuracy in reproducing experimental data, especially when considered globally on a large data set. Different classes of nuclear models can be contemplated according to their increased reliability, starting from local macroscopic approaches up to global microscopic approaches. We find in between these two extremes approaches like the classical (e.g., liquid drop, droplet), semiclassical (e.g., Thomas-Fermi), macroscopic-microscopic (e.g., classical with microscopic corrections), semi-microscopic (e.g., microscopic with phenomenological corrections), and fully microscopic (e.g., mean field, shell model) approaches. In a very schematic way,

the higher the degree of reliability, the less accurate the model used to reproduce the bulk set of experimental data. The classical or phenomenological approaches are highly parametrized and therefore often successful in reproducing experimental data or at least much more accurate than microscopic calculations. The low accuracy obtained with microscopic models mainly originates from computational complications making the determination of free parameters by fits to experimental data time-consuming. Nowadays, microscopic models can be tuned at the same level of accuracy as the phenomenological models, renormalized on experimental data if needed, and therefore could replace the phenomenological inputs little by little in applications for which nuclear properties need to be predicted.

Among the most popular global mass models, two main categories can be found, namely, *(i)* the microscopic-macroscopic approach, based on the liquid-drop model and consisting of various degrees of refinement of the original mass model of von Weizsäcker (1935), in particular by including microscopic corrections for the shell and pairing effects, and *(ii)* the relativistic or nonrelativistic mean-field approach using the density functional theory. Both approaches are described below.

## Macroscopic-Microscopic Mass Models

The very first attempt to describe theoretically nuclear binding energies goes back to the "semiempirical" mass formula of von Weizsäcker (1935). This approach corresponds to the widely used liquid-drop model of the nucleus, i.e., a macroscopic formulation which accounts for all but a small part of the variation in the binding energy. The corresponding binding energy of the spherical liquid drop is given by

$$E_{LDM} = a_v A + a_s A^{2/3} + (a_{sym} + a_{ss} A^{-1/3}) A I^2 + a_c Z^2 A^{1/3} \tag{9}$$

where $I = (N - Z)/A$. It includes the leading volume and surface terms as well as a symmetry energy (also with a volume and surface contribution) and a Coulomb energy. In particular, the liquid-drop parameters derived by Lunney et al. (2003), namely, $a_v = -15.73$, $a_s = 17.77$, $a_{sym} = 26.46$, $a_{ss} = -17.70$, and $a_c = 0.709$ (all expressed in MeV), give rise to an rms deviation of 2.98 MeV with respect to the 2457 $N, Z \geq 8$ experimental masses of 2020 AME. This rms deviation is similar to the one obtained in 2003 by their optimal fit to the 1768 masses measured at that time. With only five parameters and no microscopic corrections, it is surprisingly of similar magnitude as the one obtained with mean-field models when the interaction is adjusted only on a handful number of nuclear masses (see below).

Improvements have been brought little by little to the original liquid-drop mass formula (Eq. 9), leading to the development of macroscopic-microscopic mass formulas, where microscopic corrections to account for the quantum shell and pairing correlation effects are added to the liquid-drop part. In this framework, the macroscopic and microscopic features are treated independently, both part being connected exclusively by a parameter fit to experimental masses. Later developments included in the macroscopic part properties of infinite and semi-

infinite nuclear matter and the finite-range character of nuclear forces (for a review, see Lunney et al. 2003). The most sophisticated version of this macroscopic-microscopic mass formulas is the "finite-range droplet model" (FRDM) (Möller et al. 2016). The calculations are based on the finite-range droplet macroscopic model and the folded-Yukawa single-particle microscopic correction. The 31 independent mass-related parameters of the FRDM are determined directly from a least-squares adjustment to the ground-state masses on all the masses available at that time. This fit leads to a final rms deviation of 0.61 MeV for the 2457 $Z$, $N \geq 8$ nuclei with experimental masses. Inspired by the Skyrme energy-density functional (see below), the so-called Weizsäcker-Skyrme (WS) macroscopic-microscopic mass formula was also proposed by Wang et al. (2010, 2014) and Liu et al. (2011) with an rms deviation of about 0.3 MeV. In such an approach, the mass formula is mathematically corrected by including a Fourier spectral analysis examining the deviations of nuclear mass predictions to the experimental data at the expense of a huge increase in the number of free parameters and potentially a decrease in the predictive power of the model.

Despite the great empirical success of the macroscopic-microscopic approach, it suffers from major shortcomings, such as the incoherent link between the macroscopic part and the microscopic correction, the instability of the mass prediction to different parameter sets, or the instability of the shell correction (Pearson 2001; Lunney et al. 2003). The quality of the mass models available is traditionally estimated by the rms error obtained in the fit to experimental data and the associated number of free parameters. However, this overall accuracy does not imply a reliable extrapolation far away from the experimentally known region in view of the possible shortcomings linked to the physics theory underlying the model. As discussed above, the reliability of the mass extrapolation is a second criterion of first importance when dealing with specific applications such as astrophysics, but also more generally for the predictions of experimentally unknown ground- and excited-state properties. For this reason, microscopic mass models have been developed, as discussed below.

## Mean-Field Models

A simple unification of the liquid-drop and shell models is achieved in the Hartree-Fock (HF) method, also known as the "mean-field method" (for reviews, see, e.g., Lunney et al. 2003; Bender et al. 2003; Robledo et al. 2018). This is a variational approach in which the trial wavefunction of the nucleus has an independent particle form, i.e., it has the form of a Slater determinant $\Phi_0 = \det\{\phi_i(x_i)\}$, where the $\phi_i(x_i)$ are single-particle wavefunctions. The energy of the nucleus is then calculated by minimizing the expectation value $< \Phi_0|H^{HF}|\Phi_0 >$ with respect to arbitrary variations in the $\phi_i(x_i)$ (subject to whatever symmetries that have been imposed), while the nuclear forces appearing in the model Hamiltonian $H^{HF}$ are suitably parametrized. An essential step in this process is the calculation of the mean field for which the $\phi_i(x_i)$ are eigenfunctions, but since this mean field itself depends on

these wavefunctions, the process has to be reiterated until an acceptable level of self-consistency is reached. But wavefunctions of the form $\Phi_0$, which contain no correlations, can never be identical to the exact nuclear wavefunction corresponding to "real" nucleonic forces, no matter what the choice of the $\phi_i(x_i)$. It follows that the expectation value of the "real" nuclear Hamiltonian taken with respect to the trial function $\Phi_0$ will always be higher than the exact ground-state energy of the nucleus. Thus, if the HF method is to give the exact energy, the "real" forces need to be replaced by considerably softer "effective" forces that do not fit the nucleon-nucleon scattering data; the difference between the real and effective forces compensates, to some extent, the correlations in the real nuclear wavefunction that have been neglected in adopting the model wavefunction $\Phi_0$.

An extremely popular form of effective force is that of Skyrme, first used in the HF context by Vautherin and Brink (1972). In its usual form, this force has ten free parameters, consisting of five separate zero-range terms: a static term ($t_0$), a momentum-dependent $s$-wave term ($t_1$), a momentum-dependent $p$-wave term ($t_2$), a static density-dependent term ($t_3$), and a spin-orbit term ($W_0$). Gogny (1973) introduced another successful form of effective force consisting of several finite-range Gaussian terms (along with Skyrme-type $t_3$ and $W_0$ terms).

Since it is not possible to implicitly include some residual long-range correlations like the pairing correlations into the effective force, those must be taken explicitly into account. The simplest way to do this is to apply the BCS method (taken from the theory of superconductivity) after each HF iteration, using the current basis of single-particle states. However, the validity of the BCS approach to pairing is questionable for exotic neutron-rich nuclei; essentially because of the role played by the continuum of single-particle neutron states, it is preferable to use the computationally more demanding Hartree-Fock-Bogoliubov (HFB) method. This method is variational, like the HF method, but the pairing correlations are now built right into the trial function.

Whether one adopts the HF+BCS or HFB methods, fitting the force parameters to all the mass data is an extremely laborious process, especially when the mean field of which the $\phi_i(x_i)$ are eigenfunctions is allowed to deform, and for many years practitioners limited their fits to only a few nuclei whose sphericity was well established, usually just the doubly closed shell nuclei. Hundreds of effective interactions have been in this way published (see, e.g., Dutra et al. 2012), but since they have been fitted on a few masses only, they describe the bulk of measured masses with an rms deviation hardly better than 2–3 MeV in the best cases, i.e., hardly better than the simple five-parameter liquid-drop formula given by Eq. 9. For example, masses obtained with the SLy4 interactions give an rms deviation of the order of 5 MeV, respectively, on known masses of even-even nuclei (Stoitsov et al. 2003), and the recent UNEDF1 mass calculation (Kortelainen et al. 2012) reproduced measured values with an rms deviation of 2.1 MeV. With such a low accuracy, these masses should not be used for applications, such as the r-process nucleosynthesis.

It was only at the beginning of this century that the first complete fit to essentially all nuclei was made: this was the Skyrme-based HF+BCS mass model of Goriely

et al. (2001) with 16 parameters which gives an rms deviation of 0.785 MeV on the 2457 known masses. Subsequently, beginning with the work of Samyn et al. (2002), the Brussels-Montreal group adopted the HFB method, still using Skyrme-type forces with a contact-pairing interaction, together with phenomenological correction for the Wigner terms and the spurious collective energy within the cranking approximation (Goriely et al. 2016, and references therein). In these HFB mass models, all parameters (typically 24) are fitted to essentially all the experimental mass data. While the first HFB-1 mass model aimed at proving that it was possible to reach a low rms deviation with respect to all experimental masses available at that time, most of the subsequent models were developed to further explore the parameter space widely or to take into account additional constraints with a view to their astrophysical application in neutron-rich environments. These include in particular a sensitivity study of the mass model accuracy and extrapolation to major changes in the description of the pairing interaction, the spin-orbit coupling, or the nuclear-matter properties, such as the effective mass, the symmetry energy, and the stability of the equation of state.

With respect to the 2457 measured masses (Wang et al. 2021), the 32 HFB mass models give an rms deviation ranging between 0.52 MeV for HFB-27 and 0.82 MeV for HFB-1, as illustrated in Fig. 4. It should be noted that the fit of the Skyrme parameters to the masses was constrained by the additional condition of a simultaneous fit to the zero-temperature equation of state of homogeneous neutron
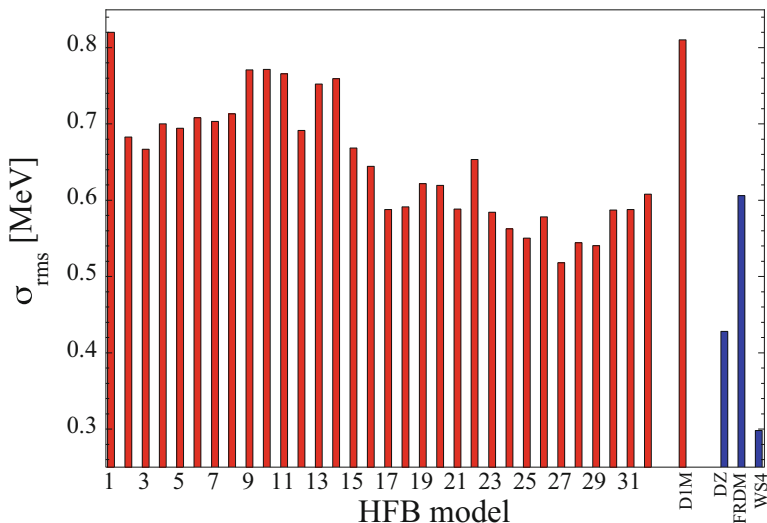


**Fig. 4** Representation of the rms deviations for the 32 Skyrme-HFB mass models, labeled from HFB-1 to HFB-32, as well as the Gogny-HFB model based on the D1M interaction, the DZ approach (Duflo and Zuker 1995), and the FRDM (Möller et al. 2016) and WS4 (Wang et al. 2014) macroscopic-microscopic formulas. The rms deviation is calculated with respect to the 2457 measured masses (Wang et al. 2021)

matter, as determined by many-body calculations with realistic two- and three-nucleon forces. At the same time, the latest HFB mass models (Goriely et al. 2016, and references therein) are based on the unconventional Skyrme force containing in addition $t_4$ and $t_5$ terms, i.e., density-dependent generalizations of the usual $t_1$ and $t_2$ terms, respectively, were able to ensure (a) an optimal fit to charge radii; (b) the stability of neutron matter and of beta-equilibrated neutron-star matter, against an unphysical polarization over the entire density range relevant to the core of neutron stars; (c) an equation of state of charge-symmetric INM that is consistent with measurements of nuclear-matter flow in heavy-ion collisions (Fantina et al. 2013); (d) a qualitatively acceptable distribution of potential energy among the four different spin-isospin channels in INM; (e) an isovector effective mass smaller than the isoscalar effective mass in charge-symmetric INM at saturation density as indicated by both experiment and many-body calculations; (f) a pairing strength compatible with realistic nuclear-matter calculations in which the self-energy corrections are included; and (g) an accurate description of fission barriers (Goriely et al. 2007). These mass tables are well adapted to all astrophysical applications, especially for the neutron-rich nuclei involved in the r-process and the outer crust of neutron stars. Since its underlying forces are likewise highly suitable for both the core and the inner crust of neutron stars, a unified treatment of all regions of neutron stars is also possible (Pearson et al. 2018).

HFB mass models can alternatively be based on Gogny-type forces, i.e., finite-range forces. In this approach, the same force is used in the pairing channel, although there is no obvious requirement that this choice be made. The only Gogny interaction leading to an accurate prediction of nuclear masses is the D1M force (Goriely et al. 2009). A special feature of this model, besides the finite-range force itself, is a much more sophisticated attempt to take account of quadrupole correlations, i.e., to restore rotational symmetry, than in the Skyrme-HFB mass models. In particular, the quadrupole collective corrections to the binding energies and nuclear radii are included in the mass model by solving the collective Schrödinger equation with the five-dimensional collective Hamiltonian consistently on the basis of the same final force that emerges from the fit.

As with the Skyrme models that we have described, D1M is subject to a neutron-matter constraint, but the equation of state of infinite neutron matter is relatively soft and would support a maximum possible neutron-star mass of 1.74 $M_\odot$. This is a problem that will have to be rectified before any definitive statement could be made concerning the suitability of Gogny forces for astrophysical applications. This issue has been addressed by Gonzalez-Boquera et al. (2019) who proposed a reparametrization of the D1M interaction. The so-called D1M* force predicts a maximum neutron star mass of 2 $M_\odot$ but at the expense of a less accurate prediction of nuclear masses. No complete mass model is however available for this interaction yet.

Concerning the precision with which D1M fits the mass data, we see from Fig. 4 that the overall quality is not as good as with Skyrme-HFB mass model, but, except from these BSk forces, D1M leads to significantly better mass predictions than the other Skyrme or Gogny interactions available and in addition does not include any

phenomenological corrections for the Wigner terms. In that sense, together with the quadrupole correction energies obtained from the collective Hamiltonian, D1M still represents the most microscopic mass model capable of reproducing the bulk of experimental masses with an rms deviation of the order of 0.8 MeV, as needed for applications.

Finally, relativistic mean-field (RMF) theory has been very successful in describing nuclear structure properties (Meng 2016), but has not reached yet the development of highly accurate mass models. Popular models like NL3 (Lalazissis et al. 1997), DD-ME2 (Lalazissis et al. 2005), or DD-ME$\delta$ (Roca-Maza et al. 2011), which were fitted to a small set of nuclei, usually exhibit an rms deviation larger than 2 MeV with respect to the full set of measured masses. In contrast, the point-coupling functional PC-PK1 including a rotational correction leads to an rms deviation of about 1.4 MeV (Hua et al. 2012). An improved description of masses has been reached by the DD-MEB1 and DD-MEB2 RMF models with density-dependent meson couplings, separable pairing, and microscopic estimations for the translational and rotational correction energies (Peña-Arteaga et al. 2016). The interactions have been fitted to essentially all experimental masses, but also to charge radii and infinite nuclear-matter properties. Both mass models describe the 2457 experimental masses with an rms deviation of about 1.2 MeV. However, these Lagrangians, like all previously determined RMF models, present the drawback of being characterized by a low effective mass, which leads to strong shell effects due to the strong coupling between the spin-orbit splitting and the effective mass.

Finally, another microscopically rooted approach worth considering is the development by Duflo and Zuker (1995, hereafter referred to as DZ) of a mass formula based on the shell model. In this approach, the nuclear Hamiltonian is separated into a monopole term and a residual multipole term. The monopole term is responsible for saturation and single-particle properties and fitted phenomenologically. The multipole part is derived from realistic interactions. Different versions of the mass formula exist with a number of free parameters ranging between 10 and 28. The version with 10 (28) free parameters reproduces the 2457 $Z$, $N \geq 8$ experimental masses with an rms error of 0.61 (0.43) MeV.

## Uncertainties in Mass Predictions

The error associated with the mass predictions comes from uncertainties affecting either the model parameters or the model itself. As mentioned above, the macroscopic-microscopic model suffers from major shortcomings, such as the incoherent link between the macroscopic part and the microscopic correction, the instability of the mass prediction to different parameter sets, or the instability of the shell correction. In particular, the deviations related to the model parameters are known to be potentially very large. An example comes from the well-known mass models of Hilf et al. (1976) and von Groote et al. (1976) based exactly on the same droplet description but making use of two possible minimizations relative to the parameter set. Their respective parameters led to very similar rms deviations
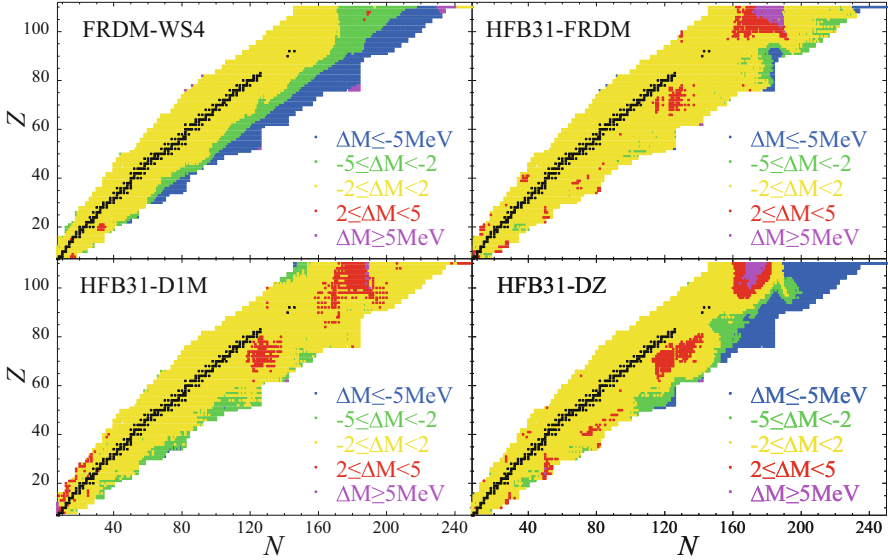
**Fig. 5** Representation in the $(N, Z)$ plane of the mass differences between HFB-31 (Goriely et al. 2016), FRDM (Möller et al. 2016), WS4 (Wang et al. 2014), and DZ (Duflo and Zuker 1995) (with 28 parameters) models for all the 8500 nuclei from $Z = 8$ up to $Z = 110$ between the HFB-31 proton and neutron driplines

from experimental masses (typically 0.75 MeV on the 1440 experimental masses known at that time), but lead to very different predictions for neutron-rich nuclei. More specifically, both fits agree within 1 MeV for stable nuclei and within 6 MeV for known unstable neutron-rich nuclei. They show complete disagreement for unknown masses. Mass differences as large as 35 MeV indeed appear for nuclei close to the neutron dripline, as shown in Goriely and Arnould (1992). Similar deviations, though less extreme, are seen in Fig. 5 where differences between the FRDM and WS4 masses close to the neutron dripline can reach up to 20 MeV, especially in the $Z = 51$–$55$ and $Z = 75$–$81$ isotopic chains. Differences are also found between the HFB and FRDM mass extrapolations, especially for heavy $N \gtrsim 180$ nuclei. A rather stronger shell effect at $N = 184$ is predicted by HFB models relative to FRDM. More discrepancies are obtained between the HFB and DZ models (Fig. 5), especially for neutron-rich and heavy or super-heavy nuclei.

Concerning the HFB mass models, when dealing with exotic nuclei far away from stability, deviations between the 32 HFB mass predictions can become significant, not only in the rigidity of the mass parabola but also in the description of the shell gaps or pairing correlations (Goriely and Capote 2014). The $1\sigma$ variance between the 32 HFB mass predictions (with respect to the HFB-24 mass model) is illustrated in Fig. 6 (lower panel) where deviations up to about 3 MeV can be found at the neutron dripline for the heaviest species. Such uncertainties can be interpreted as the model uncertainties (due to model defects) inherent to the given HFB

**Fig. 6** (Color online) Lower panel: representation in the $(N, Z)$ plane of the $1\sigma$ uncertainty corresponding to the 32 Skyrme-HFB mass models for all the 8500 nuclei included in the mass tables from $Z = 8$ up to $Z = 110$ (Goriely et al. 2016, and references therein). Upper panel: $1\sigma$ parameter uncertainty estimated through local changes of HFB-24 parameters using a weighting function $\exp[-(\chi_i^2/\chi_{min}^2)^2]$. (See Goriely and Capote 2014 for more details)
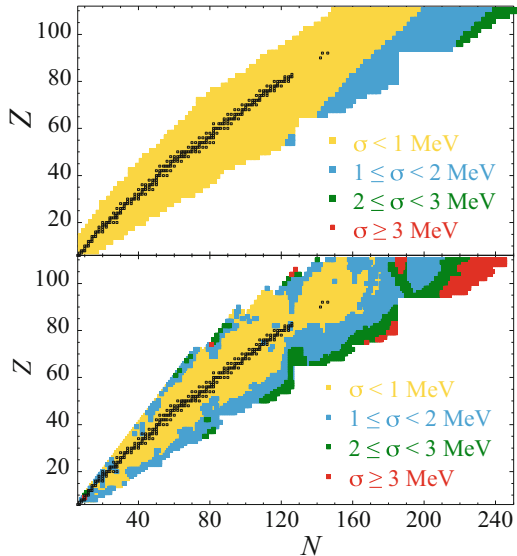
model (Neudecker et al. 2013) and are considered to be independent of parameter uncertainties. These model uncertainties have been shown to be significantly larger than the uncertainties associated with local variations of the model parameters in the vicinity of an HFB minimum (Goriely and Capote 2014), as estimated using a variant of the backward-forward Monte Carlo method (Bauge and Dossantos-Uzarralde 2011) to propagate the uncertainties on the masses of exotic nuclei far away from the experimentally known regions. The corresponding $1\sigma$ parameter uncertainties estimated for the HFB-24 mass model are given in Fig. 6 (upper panel) using a weighting function $\exp[-(\chi_i^2/\chi_{min}^2)^2]$ (where $\chi_{min}^2$ represents the minimal value of the $\chi^2$ function, i.e., the reference HFB-24 $\chi^2$). Uncertainties smaller than 2 MeV are found showing that uncertainties associated with local changes of the HFB parameters remain significantly smaller than those associated with nonlocal changes as described by the 32 HFB mass models. The large degrees of freedom offered by the 32 HFB models also allow for significantly different predictions of shell effects, pairing energies, and deformation transitions, while the statistical parameter uncertainty is restricted to the changes in the vicinity of the local minimum and consequently does not give rise to major changes of these quantities.

When considering mass models obtained in relatively different frameworks, e.g., the Skyrme-HFB or Gogny-HFB mass models, non-negligible deviations can be found in the mass extrapolations away from the experimentally known region. For example, as shown in Fig. 5, deviations up to typically $\pm 5$ MeV are found for exotic neutron-rich nuclei between HFB-31 (Goriely et al. 2016) and D1M (Goriely et al. 2009) models, especially around the $N = 126$ and 184 shell closures.

## Concluding Remarks

For more than 100 years, atomic mass spectrometry plays a crucial role not only in identifying isotopes but also to provide important input to many outstanding investigations in atomic, neutrino, astro-, and nuclear physics. Today specialized and highly developed mass-measurement systems, i.e., Penning traps, storage rings, and multi-reflection time-of-flight mass spectrometers, are being employed with increasing sensitivity and resolution. Radionuclides with half-lives as low as a few $s$ and production rates of only a few ions per minute can be addressed. On stable species relative mass uncertainties of a few $10^{-12}$ have been demonstrated, opening up the field to, e.g., particle physics and dark matter search.

Mass models have been developed mainly following two approaches, namely, macroscopic-microscopic models on the one hand and mean-field models on the other hand. Both approaches can reach rms deviations with respect to all the 2457 known masses better than typically $0.8$ MeV. Such models need also to be tested with respect to their capacity to describe not only masses but also bulk structure properties like deformations, radii, as well as infinite nuclear-matter properties. While extrapolations by macroscopic-microscopic formulas remain unstable to different parametrization, mean-field models mainly suffer from uncertainties related to the type of adopted energy-density functional and the still large range of acceptable parameters. The different approaches typically lead to extrapolations toward experimentally unknown nuclei that can deviate by more than $\sim 5$ MeV but also give rise to non-negligible variations of the pairing and shell effects. In such circumstances, neutron-capture rates in particular can be affected by 3 to 5 orders of magnitude with such mass differences, essentially due to different local variations in the pairing and shell description. Such deviations by far exceed what is acceptable for nucleosynthesis applications. For this reason, further improvements of the mass model are needed. These include development of relativistic as well as nonrelativistic mean-field models, but also the explicit inclusion within such approaches of the state-of-the-art corrections, like the quadrupole or octupole correlations by the generator coordinate method and a proper treatment of odd-$A$ and odd-odd nuclei with time-reversal symmetry breaking. Such models should reproduce not only nuclear masses at best but also as many experimental observables as possible. These include charge radii and neutron skin thicknesses, fission barriers and shape isomers, spectroscopic data such as the $2^+$ energies, moments of inertia, but also infinite (neutron and symmetric) nuclear-matter properties obtained from realistic calculations as well as specific observed or empirical properties of neutron stars, like their maximum mass or mass-radius relations.

## References

D.S. Ahn, N. Fukuda, H. Geissel, N. Inabe, N. Iwasa, T. Kubo, K. Kusaka, D.J. Morrissey, D. Murai, T. Nakamura, M. Ohtake, H. Otsu, H. Sato, B.M. Sherrill, Y. Shimizu, H. Suzuki, H. Takeda, O.B. Tarasov, H. Ueno, Y. Yanagisawa, K. Yoshida, Location of the neutron dripline at fluorine and neon. Phys. Rev. Lett. **123**, 212501 (2019)

M. Aker, K. Altenmüller, A. Beglarian, J. Behrens, A. Berlev, U. Besserer, B. Bieringer, K. Blaum,
    F. Block, B. Bornschein, L. Bornschein, M. Böttcher, T. Brunst, T.S. Caldwell, L. La Cascio,
    S. Chilingaryan, W. Choi, D. Díaz Barrero, K. Debowski, M. Deffert, M. Descher, P.J. Doe,
    O. Dragoun, G. Drexlin, S. Dyba, F. Edzards, K. Eitel, E. Ellinger, R. Engel, S. Enomoto, M.
    Fedkevych, A. Felden, J.A. Formaggio, F.M. Fränkle, G.B. Franklin, F. Friedel, A. Fulst, K.
    Gauda, W. Gil, F. Glück, R. Grössle, R. Gumbsheimer, T. Höhn, V. Hannen, N. Haußmann, K.
    Helbing, S. Hickford, R. Hiller, D. Hilesheimer, D. Hinz, T. Houdy, A. Huber, A. Jansen, L.
    Köllenberger, C. Karl, J. Kellerer, L. Kippenbrock, M. Klein, A. Kopmann, M. Korzeczek, A.
    Kovalík, B. Krasch, H. Krause, T. Lasserre, T.L. Le, O. Lebeda, B. Lehnert, A. Lokhov, J.M.
    Lopez Poyato, K. Müller, M. Machatschek, E. Malcherek, M. Mark, A. Marsteller, E.L. Martin,
    C. Melzer, S. Mertens, S. Niemes, P. Oelpmann, A. Osipowicz, D.S. Parno, A.W.P. Poon, F.
    Priester, M. Röllig, C. Röttele, O. Rest, R.G.H. Robertson, C. Rodenbeck, M. Ryšavý, R. Sack,
    A. Saenz, A. Schaller (née Pollithy), P. Schäfer, L. Schimpf, K. Schlösser, M. Schlösser, L.
    Schlüter, M. Schrank, B. Schulz, M. Ščík, H. Seitz-Moskaliuk, V. Sibille, D. Siegmann, M.
    Slezák, F. Spanier, M. Steidl, M. Sturm, M. Sun, H.H. Telle, T. Thümmler, L.A. Thorne, N.
    Titov, I. Tkachev, N. Trost, D. Vénos, K. Valerius, A.P. Vizcaya Hernández, S. Wüstling, M.
    Weber, C. Weinheimer, C. Weiss, S. Welte, J. Wendel, J.F. Wilkerson, J. Wolf, W. Xu, Y.-R.
    Yen, S. Zadoroghny, G. Zeller, Analysis methods for the first katrin neutrino-mass measurement.
    Phys. Rev. D **104**, 012005 (2021)
B. Alpert, M. Balata, D. Bennett, M. Biasotti, C. Boragno, C. Brofferio, V. Ceriale, D. Corsini,
    P.K. Day, M. De Gerone, R. Dressler, M. Faverzani, E. Ferri, J. Fowler, F. Gatti, A. Giachero,
    J. Hays-Wehle, S. Heinitz, G. Hilton, U. Köster, M. Lusignoli, M. Maino, J. Mates, S. Nisi,
    R. Nizzolo, A. Nucciotti, G. Pessina, G. Pizzigoni, A. Puiu, S. Ragazzi, C. Reintsema, M.R.
    Gomes, D. Schmidt, D. Schumann, M. Sisti, D. Swetz, F. Terranova, J. Ullom, Holmes – the
    electron capture decay of $^{163}$ho to measure the electron neutrino mass with sub-ev sensitivity.
    Eur. Phys. J. C **75**, 112 (2015)
M. Arnould, S. Goriely, The p-process of stellar nucleosynthesis: astrophysics and nuclear physics
    status. Phys. Rep. **384**, 1–84 (2003)
M. Arnould, S. Goriely, Astronuclear physics: a tale of the atomic nuclei in the skies. Prog. Part.
    Nucl. Phys. **112**, 103766 (2020)
M. Arnould, S. Goriely, K. Takahashi, The r-process of stellar nucleosynthesis: astrophysics and
    nuclear physics achievements and mysteries. Phys. Rep. **450**, 97 (2007)
D. Atanasov, P. Ascher, K. Blaum, R.B. Cakirli, T.E. Cocolios, S. George, S. Goriely, F. Herfurth,
    H.-T. Janka, O. Just, M. Kowalska, S. Kreim, D. Kisler, Y.A. Litvinov, D. Lunney, V. Manea,
    D. Neidherr, M. Rosenbusch, L. Schweikhard, A. Welker, F. Wienholtz, R.N. Wolf, K. Zuber,
    Precision mass measurements of $^{129--131}$Cd and their impact on stellar nucleosynthesis via the
    rapid neutron capture process. Phys. Rev. Lett. **115**, 232501 (2015)
F.T. Avignone, S.R. Elliott, J. Engel, Double beta decay, majorana neutrinos, and neutrino mass.
    Rev. Mod. Phys. **80**, 481–516 (2008)
A.S. Barabash, *Brief Review of Double Beta Decay Experiments* (2017)
E. Bauge, P. Dossantos-Uzarralde, Evaluation of the covariance matrix of 239pu neutronic cross
    sections in the continuum using the backward-forward Monte-Carlo method. J. Korean Phys.
    Soc. **59**, 1218 (2011)
M. Bender, P.-H. Heenen, P.-G. Reinhard, Self-consistent mean-field models for nuclear structure.
    Rev. Mod. Phys. **75**, 121–180 (2003)
B. Blank, M. Płoszajczak, Two-proton radioactivity. Rep. Progress Phys. **71**, 046301 (2008)
K. Blaum, J. Dilling, W. Noertershauser, Precision atomic physics techniques for nuclear physics
    with radioactive beams. Phys. Scripta **T152**, 014017 (2013)
K. Blaum, S. Eliseev, F.A. Danevich, V.I. Tretyak, S. Kovalenko, M.I. Krivoruchenko, Y.N.
    Novikov, J. Suhonen, Neutrinoless double-electron capture. Rev. Mod. Phys. **92**, 045007 (2020)
A. Bohr, B.R. Mottelson, *Nuclear Structure*, vol. II (World Scientific Publishing Co. Pte. Ltd.,
    1998). ISBN 9810239807
G. Bollen, P. Dabkiewicz, P. Egelhof, T. Hilberath, H. Kalinowsky, F. Kern, H. Schnatz, L.
    Schweikhard, H. Stolzenberg, R.B. Moore, H.-J. Kluge, G.M. Temmer, G. Ulm, First absolute
    mass measurements of short-lived isotopes. Hyperfine Interact. **38**, 793–802 (1987)

G. Bollen, H.J. Kluge, T. Otto, G. Savard, H. Stolzenberg, Ramsey technique applied in a penning trap mass spectrometer. Nucl. Inst. Methods Phys. Res. B **70**, 490–493 (1992)

A.E. Cameron, D.F. Eggers, An ion "velocitron". Rev. Sci. Instrum. **19**, 605–607 (1948)

L. Canete, S. Giraud, A. Kankainen, B. Bastin, F. Nowacki, A. Poves, P. Ascher, T. Eronen, V. Alcindor, A. Jokinen, A. Khanam, I.D. Moore, D.A. Nesterenko, F. De Oliveira Santos, H. Penttilä, C. Petrone, I. Pohjalainen, A. de Roubin, V.A. Rubchenya, M. Vilen, J. Äystö, Precision mass measurements of $^{67}$Fe and $^{69,70}$Co: nuclear structure toward $n = 40$ and impact on $r$-process reaction rates. Phys. Rev. C **101**, 041304 (2020)

R. Capote, M. Herman, P. Oblozinsky, P.G. Young, S. Goriely, T. Belgya, A.V. Ignatyuk, A.J. Koning, S. Hilaire, V.A. Plujko, M. Avrigeanu, O. Bersillon, M.B. Chadwick, T. Fukahori, Z. Ge, Y. Han, S. Kailas, J. Kopecky, V.M. Maslov, G. Reffo, M. Sin, E.S. Soukhovitskii, P. Talou, Reference input parameter library (ripl-3). Nucl. Data Sheets **110**, 3107 (2009)

E. Caurier, G. Martínez-Pinedo, F. Nowacki, A. Poves, A.P. Zuker, The shell model as a unified view of nuclear structure. Rev. Mod. Phys. **77**, 427–488 (2005)

A. Chaudhuri, C. Andreoiu, T. Brunner, U. Chowdhury, S. Ettenauer, A.T. Gallant, G. Gwinner, A.A. Kwiatkowski, A. Lennarz, D. Lunney, T.D. Macdonald, B.E. Schultz, M.C. Simon, V.V. Simon, J. Dilling, Evidence for the extinction of the $n = 20$ neutron-shell closure for $^{32}$mg from direct mass measurements. Phys. Rev. C **88**, 054317 (2013)

P. Chauveau, P. Delahaye, G. De France, S. El Abir, J. Lory, Y. Merrer, M. Rosenbusch, L. Schweikhard, R.N. Wolf, Pilgrim, a multi-reflection time-of-flight mass spectrometer for spiral2-s3 at ganil. Nucl. Instrum. Methods Phys. Res. Sect. B: Beam Interact. Mater. Atoms **376**, 211–215 (2016)

A. Choplin, R. Hirschi, G. Meynet, S. Ekström, C. Chiappini, A. Laird, Non-standard s-process in massive rotating stars. Astron. Astrophys. **618**, A133 (2018)

U. Chowdhury, K.G. Leach, C. Andreoiu, A. Bader, M. Brodeur, A. Chaudhuri, A.T. Gallant, A. Grossheim, G. Gwinner, R. Klawitter, A.A. Kwiatkowski, A. Lennarz, T.D. Macdonald, J. Pearkes, B.E. Schultz, J. Dilling, First direct mass measurement of the neutron-deficient nucleus $^{24}$Al. Phys. Rev. C **92**, 045803 (2015)

J.J. Cowan, C. Sneden, J.E. Lawler, A. Aprahamian, M. Wiescher, K. Langanke, G. Martínez-Pinedo, F.-K. Thielemann, Origin of the heaviest elements: The rapid neutron-capture process. Rev. Mod. Phys. **93**, 015002 (2021)

T. Dickel, W.R. Plaß, A. Becker, U. Czok, H. Geissel, E. Haettner, C. Jesch, W. Kinsel, M. Petrick, C. Scheidenberger, A. Simon, M.I. Yavor, A high-performance multiple-reflection time-of-flight mass spectrometer and isobar separator for the research with exotic nuclei. Nucl. Instrum. Methods Phys. Res. Sect. A: Accel. Spectrom. Detect. Assoc. Equip. **777**, 172–188 (2015)

J. Dilling, D. Ackermann, J. Bernard, F.P. Hessberger, S. Hofmann, W. Hornung, H.J. Kluge, E. Lamour, M. Maier, R. Mann, G. Marx, R.B. Moore, G. Münzenberg, W. Quint, D. Rodriguez, M. Schüdel, J. Schönfelder, G. Sikler, C. Toader, L. Vermeeren, C. Weber, G. Bollen, O. Engels, D. Habs, P. Thirolf, H. Backe, A. Dretzke, W. Lauth, W. Ludolphs, M. Sewtz, The shiptrap project: a capture and storage facility at gsi for heavy radionuclides from ship. Hyperfine Interact. **127**, 491–496 (2000)

J. Dilling, P. Bricault, M. Smith, H.-J. Kluge, The proposed titan facility at ISAC for very precise mass measurements on highly charged short-lived isotopes. Nucl. Instrum. Methods Phys. Res. Sect. B: Beam Interact. Mater. Atoms **204**, 492–496 (2003)

J. Dilling, K. Blaum, M. Brodeur, S. Eliseev, Penning-trap mass measurements in atomic and nuclear physics. Ann. Rev. Nucl. Part. Sci. **68**, 45–74 (2018)

J. Duflo, A. Zuker, Microscopic mass formulas. Phys. Rev. C **52**, 23 (1995)

M. Dutra, O. Lourenço, J.S.S. Martins, A. Delfino, J.R. Stone, P.D. Stevenson, Skyrme interaction and nuclear matter constraints. Phys. Rev. C **85**, 035201 (2012)

A.S. Eddington, The internal constitution of the stars. Nature **106**, 14 (1920)

S. Eliseev, M. Block, A. Chaudhuri, F. Herfurth, H.-J. Kluge, A. Martin, C. Rauth, G. Vorobjev, Octupolar excitation of ions stored in a penning trap mass spectrometer – a study performed at shiptrap. Int. J. Mass Spectrom. **262**, 45–50 (2007)

S. Eliseev, M. Goncharov, K. Blaum, M. Block, C. Droese, F. Herfurth, E. Minaya Ramirez, Y.N. Novikov, L. Schweikhard, V.M. Shabaev, I.I. Tupitsyn, K. Zuber, N.A. Zubova, Multiple-resonance phenomenon in neutrinoless double-electron capture. Phys. Rev. C **84**, 012501 (2011a)

S. Eliseev, C. Roux, K. Blaum, M. Block, C. Droese, F. Herfurth, H.-J. Kluge, M.I. Krivoruchenko, Y.N. Novikov, E. Minaya Ramirez, L. Schweikhard, V.M. Shabaev, F. Šimkovic, I.I. Tupitsyn, K. Zuber, N.A. Zubova, Resonant enhancement of neutrinoless double-electron capture in $^{152}$Gd. Phys. Rev. Lett. **106**, 052504 (2011b)

S. Eliseev, K. Blaum, M. Block, C. Droese, M. Goncharov, E. Minaya Ramirez, D.A. Nesterenko, Y.N. Novikov, L. Schweikhard, Phase-imaging ion-cyclotron-resonance measurements for short-lived nuclides. Phys. Rev. Lett. **110**, 082501 (2013)

S. Eliseev, K. Blaum, M. Block, A. Dörr, C. Droese, T. Eronen, M. Goncharov, M. Höcker, J. Ketter, E.M. Ramirez, D.A. Nesterenko, Y.N. Novikov, L. Schweikhard, A phase-imaging technique for cyclotron-frequency measurements. Appl. Phys. B **114**, 107–128 (2014)

S. Eliseev, K. Blaum, M. Block, S. Chenmarev, H. Dorrer, C.E. Düllmann, C. Enss, P.E. Filianin, L. Gastaldo, M. Goncharov, U. Köster, F. Lautenschläger, Y.N. Novikov, A. Rischka, R.X. Schüssler, L. Schweikhard, A. Türler, Direct measurement of the mass difference of $^{163}$Ho and $^{163}$Dy solves the $q$-value puzzle for the neutrino mass determination. Phys. Rev. Lett. **115**, 062501 (2015a)

S. Eliseev, K. Blaum, M. Block, S. Chenmarev, H. Dorrer, C.E. Düllmann, C. Enss, P.E. Filianin, L. Gastaldo, M. Goncharov, U. Köster, F. Lautenschläger, Y.N. Novikov, A. Rischka, R.X. Schüssler, L. Schweikhard, A. Türler, Direct measurement of the mass difference of $^{163}$Ho and $^{163}$Dy solves the $q$-value puzzle for the neutrino mass determination. Phys. Rev. Lett. **115**, 062501 (2015b)

T. Eronen, V.S. Kolhinen, V.-V. Elomaa, D. Gorelov, U. Hager, J. Hakala, A. Jokinen, A. Kankainen, P. Karvonen, S. Kopecky, I.D. Moore, H. Penttilä, S. Rahaman, S. Rinta-Antila, J. Rissanen, A. Saastamoinen, J. Szerypo, C. Weber, J. Äystö, Jyfltrap: a penning trap for precision mass spectroscopy and isobaric purification. Eur. Phys. J. A **48**, 46 (2012)

A.A. Esfahani, D.M. Asner, S. Bäßer, R. Cervantes, C. Claessens, L. de Viveiros, P.J. Doe, S. Doeleman, J.L. Fernandes, M. Fertl, E.C. Finn, J.A. Formaggio, D. Furse, M. Guigue, K.M. Heeger, A.M. Jones, K. Kazkaz, J.A. Kofron, C. Lamb, B.H. LaRoque, E. Machado, E.L. McBride, M.L. Miller, B. Monreal, P. Mohanmurthy, J.A. Nikkel, N.S. Oblath, W.C. Pettus, R.G.H. Robertson, L.J. Rosenberg, G. Rybka, D. Rysewyk, L. Saldaña, P.L. Slocum, M.G. Sternberg, J.R. Tedeschi, T. Thümmler, B.A. VanDevender, L.E. Vertatschitsch, M. Wachtendonk, J. Weintroub, N.L. Woods, A. Young, E.M. Zayas, Determining the neutrino mass with cyclotron radiation emission spectroscopy—project 8 **44**, 054004 (2017)

J. Fallis, J.A. Clark, K.S. Sharma, G. Savard, F. Buchinger, S. Caldwell, A. Chaudhuri, J.E. Crawford, C.M. Deibel, S. Gulick, A.A. Hecht, D. Lascar, J.K.P. Lee, A.F. Levand, G. Li, B.F. Lundgren, A. Parikh, S. Russell, M. Scholte-van de Vorst, N.D. Scielzo, R.E. Segel, H. Sharma, S. Sinha, M.G. Sternberg, T. Sun, I. Tanihata, J. Van Schelt, J.C. Wang, Y. Wang, C. Wrede, Z. Zhou, Mass measurements of isotopes of nb, mo, tc, ru, and rh along the $\nu p$- and $rp$-process paths using the canadian penning trap mass spectrometer. Phys. Rev. C **84**, 045807 (2011)

A.F. Fantina, J.M.P.N. Chamel, S. Goriely, Neutron star properties with unified equations of state of dense matter. Astron. Astrophys. **559**, 128 (2013)

P. Filianin, C. Lyu, M. Door, K. Blaum, W.J. Huang, M. Haverkort, P. Indelicato, C.H. Keitel, K. Kromer, D. Lange, Y.N. Novikov, A. Rischka, R.X. Schüssler, C. Schweiger, S. Sturm, S. Ulmer, Z. Harman, S. Eliseev, Direct $q$-value determination of the $\beta^-$ decay of $^{187}$Re. Phys. Rev. Lett. **127**, 072502 (2021)

J.A. Formaggio, A.L.C. de Gouvêa, R.G.H. Robertson, Direct measurements of neutrino mass. Phys. Rep. **914**, 1–54 (2021)

B. Franzke, The heavy ion storage and cooler ring project ESR at GSI. Nucl. Instrum. Methods Phys. Res. Sect. B: Beam Interact. Mater. Atoms **24–25**, 18–25 (1987)

B. Franzke, H. Geissel, G. Münzenberg, Mass and lifetime measurements of exotic nuclei in storage rings. Mass Spectrom. Rev. **27**, 428–469 (2008)

Y. Fukuda, T. Hayakawa, E. Ichihara, K. Inoue, K. Ishihara, H. Ishino, Y. Itow, T. Kajita, J. Kameda, S. Kasuga, K. Kobayashi, Y. Kobayashi, Y. Koshio, M. Miura, M. Nakahata, S. Nakayama, A. Okada, K. Okumura, N. Sakurai, M. Shiozawa, Y. Suzuki, Y. Takeuchi, Y. Totsuka, S. Yamada, M. Earl, A. Habig, E. Kearns, M.D. Messier, K. Scholberg, J.L. Stone, L.R. Sulak, C.W. Walter, M. Goldhaber, T. Barszczak, D. Casper, W. Gajewski, P.G. Halverson, J. Hsu, W.R. Kropp, L.R. Price, F. Reines, M. Smy, H.W. Sobel, M.R. Vagins, K.S. Ganezer, W.E. Keig, R.W. Ellsworth, S. Tasaka, J.W. Flanagan, A. Kibayashi, J.G. Learned, S. Matsuno, V.J. Stenger, D. Takemori, T. Ishii, J. Kanzaki, T. Kobayashi, S. Mine, K. Nakamura, K. Nishikawa, Y. Oyama, A. Sakai, M. Sakuda, O. Sasaki, S. Echigo, M. Kohama, A.T. Suzuki, T.J. Haines, E. Blaufuss, B.K. Kim, R. Sanford, R. Svoboda, M.L. Chen, Z. Conner, J.A. Goodman, G.W. Sullivan, J. Hill, C.K. Jung, K. Martens, C. Mauger, C. McGrew, E. Sharkey, B. Viren, C. Yanagisawa, W. Doki, K. Miyano, H. Okazawa, C. Saji, M. Takahata, Y. Nagashima, M. Takita, T. Yamaguchi, M. Yoshida, S.B. Kim, M. Etoh, K. Fujita, A. Hasegawa, T. Hasegawa, S. Hatakeyama, T. Iwamoto, M. Koga, T. Maruyama, H. Ogawa, J. Shirai, A. Suzuki, F. Tsushima, M. Koshiba, M. Nemoto, K. Nishijima, T. Futagami, Y. Hayato, Y. Kanaya, K. Kaneyuki, Y. Watanabe, D. Kielczewska, R.A. Doyle, J.S. George, A.L. Stachyra, L.L. Wai, R.J. Wilkes, K.K. Young, Evidence for oscillation of atmospheric neutrinos. Phys. Rev. Lett. **81**, 1562–1567 (1998)

W.H. Furry, On transition probabilities in double beta-disintegration. Phys. Rev. **56**, 1184–1193 (1939)

G. Gamow, Mass defect curve and nuclear constitution. Proc. R. Soc. Lond. A **126**, 632–644 (1930)

L. Gastaldo, K. Blaum, K. Chrysalidis, T. Day Goodacre, A. Domula, M. Door, H. Dorrer, C.E. Düllmann, K. Eberhardt, S. Eliseev, C. Enss, A. Faessler, P. Filianin, A. Fleischmann, D. Fonnesu, L. Gamer, R. Haas, C. Hassel, D. Hengstler, J. Jochum, K. Johnston, U. Kebschull, S. Kempf, T. Kieck, U. Köster, S. Lahiri, M. Maiti, F. Mantegazzini, B. Marsh, P. Neroutsos, Y.N. Novikov, P.C.O. Ranitzsch, S. Rothe, A. Rischka, A. Saenz, O. Sander, F. Schneider, S. Scholl, R.X. Schüssler, C. Schweiger, F. Simkovic, T. Stora, Z. Szücs, A. Türler, M. Veinhard, M. Weber, M. Wegner, K. Wendt, K. Zuber, The electron capture in 163ho experiment – echo. Eur. Phys. J. Spec. Top. **226**, 1623–1694 (2017)

H. Geissel, K. Beckert, F. Bosch, H. Eickhoff, B. Franczak, B. Franzke, M. Jung, O. Klepper, R. Moshammer, G. Münzenberg, F. Nickel, F. Nolden, U. Schaaf, C. Scheidenberger, P. Spädtke, M. Steck, K. Sümmerer, A. Magel, First storage and cooling of secondary heavy-ion beams at relativistic energies. Phys. Rev. Lett. **68**, 3412–3415 (1992)

S. George, K. Blaum, F. Herfurth, A. Herlert, M. Kretzschmar, S. Nagy, S. Schwarz, L. Schweikhard, C. Yazidjian, The ramsey method in high-precision mass spectrometry with penning traps: experimental results. Int. J. Mass Spectrom. **264**, 110–121 (2007)

D. Gogny, Hartree-Fock Bogolyubov method with density-dependent interaction, in *Proceedings of the International Conference on Nuclear Physics*, ed. by J. de Boer, H.J. Mang (1973), p. 48

C. Gonzalez-Boquera, M. Centelles, X. Viñas, L.M. Robledo, New gogny interaction suitable for astrophysical applications. Eur. Phys. J. A **55**, 150 (2019)

S. Goriely, M. Arnould, The r-process in the light of a microscopic model for nuclear masses. Astron. Astrophys. **262**, 73 (1992)

S. Goriely, R. Capote, Hartree-fock-bogolyubov mass models and the uncertainties in their mass extrapolation. Phys. Rev. C **89**, 054318 (2014)

S. Goriely, L. Siess, Sensitivity of the s-process nucleosynthesis in AGB stars to the overshoot model. A&A **609**, A29 (2018)

S. Goriely, F. Tondeur, J.M. Pearson, A Hartree-Fock nuclear mass table. At. Data Nucl. Data Tables **77**, 311 (2001)

S. Goriely, M. Samyn, M.J. Pearson, Further explorations of skyrme-hartree-fock-bogoliubov mass formulas. VII. Simultaneous fits to masses and fission barriers. Phys. Rev. C **75**, 064312 (2007)

S. Goriely, S. Hilaire, M. Girod, S. Péru, First gogny hatree-fock-bogoliubov nuclear mass model. Phys. Rev. Lett. **102**, 242501–242504 (2009)

S. Goriely, A. Bauswein, H.-T. Janka, r-process nucleosynthesis in dynamically ejected matter of neutron star mergers. Astrophys. J. Lett. **738**, L32 (2011)

S. Goriely, N. Chamel, J.M. Pearson, Further explorations of skyrme-hartree-fock-bogoliubov mass formulas. XVI: Inclusion of self-energy effects in pairing. Phys. Rev. C **93**, 034337 (2016)

G. Gräff, H. Kalinowsky, J. Traut, A direct determination of the proton electron mass ratio. Zeitschrift fÃ¼r Physik A Atoms and Nuclei **297**, 35–39 (1980)

E. Haettner, D. Ackermann, G. Audi, K. Blaum, M. Block, S. Eliseev, T. Fleckenstein, F. Herfurth, F.P. Heßberger, S. Hofmann, J. Ketelaer, J. Ketter, H.-J. Kluge, G. Marx, M. Mazzocco, Y.N. Novikov, W.R. Plaß, S. Rahaman, T. Rauscher, D. Rodríguez, H. Schatz, C. Scheidenberger, L. Schweikhard, B. Sun, P.G. Thirolf, G. Vorobjev, M. Wang, C. Weber, Mass measurements of very neutron-deficient mo and tc isotopes and their impact on $rp$ process nucleosynthesis. Phys. Rev. Lett. **106**, 122501 (2011)

J.C. Hardy, I.S. Towner, Superallowed $0^+ \rightarrow 0^+$ nuclear $\beta$ decays: 2020 critical survey, with implications for $V_{ud}$ and CKM unitarity. Phys. Rev. C **102**, 045501 (2020)

D.J. Hartley, F.G. Kondev, R. Orford, J.A. Clark, G. Savard, A.D. Ayangeakaa, S. Bottoni, F. Buchinger, M.T. Burkey, M.P. Carpenter, P. Copp, D.A. Gorelov, K. Hicks, C.R. Hoffman, C. Hu, R.V.F. Janssens, J.W. Klimes, T. Lauritsen, J. Sethi, D. Seweryniak, K.S. Sharma, H. Zhang, S. Zhu, Y. Zhu, Masses and $\beta$-decay spectroscopy of neutron-rich odd-odd $^{160,162}$Eu nuclei: evidence for a subshell gap with large deformation at $n = 98$. Phys. Rev. Lett. **120**, 182502 (2018)

H. Hergert, A guided tour of ab initio nuclear many-body theory. Front. Phys. **8**, 379 (2020)

E.R. Hilf, H. von Groote, K. Takahashi, Gross theory of nuclear masses and radii, in *Proceedings of Third International Conference on Nuclei Far from Stability*, CERN, vol. 76–13 (1976), p. 142

T.Y. Hirsh, N. Paul, M. Burkey, A. Aprahamian, F. Buchinger, S. Caldwell, J.A. Clark, A.F. Levand, L.L. Ying, S.T. Marley, G.E. Morgan, A. Nystrom, R. Orford, A.P. Galván, J. Rohrer, G. Savard, K.S. Sharma, K. Siegl, First operation and mass separation with the caribu MR-ToF. Nucl. Instrum. Methods Phys. Res. Sect. B: Beam Interact. Mater. Atoms **376**, 229–232 (2016)

X.M. Hua, T.H. Heng, Z.M. Niu, B.H. Sun, J.Y. Guo, Comparative study of nuclear masses in the relativistic mean-field model. Sci. China-Phys. Mech. Astron. **55**, 2414 (2012)

Y. Ito, P. Schury, M. Wada, S. Naimi, T. Sonoda, H. Mita, F. Arai, A. Takamine, K. Okada, A. Ozawa, H. Wollnik, Single-reference high-precision mass measurement with a multireflection time-of-flight mass spectrograph. Phys. Rev. C **88**, 011306 (2013)

H.-T. Janka, *Handbook of Supernovae* (Springer, Cham, 2017)

A.S. Jensen, K. Riisager, D.V. Fedorov, E. Garrido, Structure and reactions of quantum halos. Rev. Mod. Phys. **76**, 215–261 (2004)

C. Jesch, T. Dickel, W.R. PlaÃŸ, D. Short, S. Ayet San Andres, J. Dilling, H. Geissel, F. Greiner, J. Lang, K.G. Leach, W. Lippert, C. Scheidenberger, M.I. Yavor, The MR-ToF-MS isobar separator for the titan facility at triumf. Hyperfine Interact. **235**, 97–106 (2015)

O. Just, A. Bauswein, R. Ardevol Pulpillo, S. Goriely, H.-T. Janka, Comprehensive nucleosynthesis analysis for ejecta of compact binary mergers. Mon. Not. R. Astron. Soc. **448**, 541 (2015).

A.I. Karakas, Updated stellar yields from asymptotic giant branch models. Mon. Not. R. Astron. Soc. **403**, 1413 (2010)

J. Ketelaer, J. Krämer, D. Beck, K. Blaum, M. Block, K. Eberhardt, G. Eitel, R. Ferrer, C. Geppert, S. George, F. Herfurth, J. Ketter, S. Nagy, D. Neidherr, R. Neugart, W. Nörtershäuser, J. Repp, C. Smorra, N. Trautmann, C. Weber, Triga-spec: a setup for mass spectrometry and laser spectroscopy at the research reactor triga mainz. Nucl. Instrum. Methods Phys. Res. Sect. A: Accel. Spectrom. Detectors Assoc. Equip. **594**, 162–177 (2008)

R. Klawitter, A. Bader, M. Brodeur, U. Chowdhury, A. Chaudhuri, J. Fallis, A.T. Gallant, A. Grossheim, A.A. Kwiatkowski, D. Lascar, K.G. Leach, A. Lennarz, T.D. Macdonald, J. Pearkes, S. Seeraji, M.C. Simon, V.V. Simon, B.E. Schultz, J. Dilling, Mass measurements of neutron-rich rb and sr isotopes. Phys. Rev. C **93**, 045807 (2016)

H.-J. Kluge, G. Bollen, Isoltrap: A tandem penning trap mass spectrometer for radioactive isotopes. Hyperfine Interact. **81**, 15–26 (1993)

M. König, G. Bollen, H.-J. Kluge, T. Otto, J. Szerypo, Quadrupole excitation of stored ion motion at the true cyclotron frequency. Int. J. Mass Spectrom. Ion Process. **142**, 95–116 (1995)

C. Kobayashi, A.I. Karakas, M. Lugaro, The origin of elements from carbon to uranium. Astrophys. J. **900**, 179 (2020)

M. Kortelainen, J. McDonnell, W. Nazarewicz, P.-G. Reinhard, J. Sarich, N. Schunck, M.V. Stoitsov, S.M. Wild, Nuclear energy density optimization: large deformations. Phys. Rev. C **85**, 024304 (2012)

M. Kretzschmar, The ramsey method in high-precision mass spectrometry with penning traps: theoretical foundations. Int. J. Mass Spectrom. **264**, 122–145 (2007)

G.A. Lalazissis, J. König, P. Ring, New parametrization for the lagrangian density of relativistic mean field theory. Phys. Rev. C **55**, 540 (1997)

G.A. Lalazissis, T. Nikšić, D. Vretenar, P. Ring, New relativistic mean-field interaction with density-dependent meson-nucleon couplings. Phys. Rev. C **71**, 024312 (2005)

M. Liu, N. Wang, Y.G. Deng, X.Z. Wu, Further improvements on a global nuclear mass model. Phys. Rev. C **84**, 014333 (2011)

D. Lunney, New mass measurements with trapped (radioactive) ions and related fundamental physics. Hyperfine Interact. **240**, 48 (2019)

D. Lunney, J.M. Pearson, C. Thibault, Recent trends in the determination of nuclear masses. Rev. Mod. Phys. **75**(3), 1021 (2003)

E.M. Lykiardopoulou, C. Izzo, E. Leistenschneider, A.A. Kwiatkowski, J. Dilling, Towards high precision mass measurements of highly charged ions using the phase-imaging ion-cyclotron-resonance technique at titan. Hyperfine Interact. **241**, 37 (2020)

V. Manea, J. Karthein, D. Atanasov, M. Bender, K. Blaum, T.E. Cocolios, S. Eliseev, A. Herlert, J.D. Holt, W.J. Huang, Y.A. Litvinov, D. Lunney, J. Menéndez, M. Mougeot, D. Neidherr, L. Schweikhard, A. Schwenk, J. Simonis, A. Welker, F. Wienholtz, K. Zuber, First glimpse of the $n = 82$ shell closure below $z = 50$ from masses of neutron-rich cadmium isotopes and isomers. Phys. Rev. Lett. **124**, 092502 (2020)

J. Meng (ed.), *Relativistic Density Functional for Nuclear Structure*, vol. 10 (World Scientific, Singapore, 2016)

B.D. Metzger, G. Martínez-Pinedo, S. Darbha, E. Quataert, A. Arcones, D. Kasen, R. Thomas, P. Nugent, I.V. Panov, N.T. Zinner, Electromagnetic counterparts of compact object mergers powered by the radioactive decay of r-process nuclei. Mon. Not. R. Astron. Soc. **406**, 2650 (2010)

P. Möller, A.J. Sierk, T. Ichikawa, H. Sagawa, Nuclear ground-state masses and deformations: FRDM (2012). At. Data Nucl. Data Tables **109–110**, 1 (2016)

E.G. Myers, A. Wagner, H. Kracke, B.A. Wesson, Atomic masses of tritium and helium-3. Phys. Rev. Lett. **114**, 013003 (2015)

D.A. Nesterenko, S. Eliseev, K. Blaum, M. Block, S. Chenmarev, A. Dörr, C. Droese, P.E. Filianin, M. Goncharov, E. Minaya Ramirez, Y.N. Novikov, L. Schweikhard, V.V. Simon, Direct determination of the atomic mass difference of $^{187}$Re and $^{187}$Os for neutrino physics and cosmochronology. Phys. Rev. C **90**, 042501 (2014)

D.A. Nesterenko, T. Eronen, A. Kankainen, L. Canete, A. Jokinen, I.D. Moore, H. Penttilä, S. Rinta-Antila, A. de Roubin, M. Vilen, Phase-imaging ion-cyclotron-resonance technique at the jyfltrap double penning trap mass spectrometer. Eur. Phys. J. A **54**, 154 (2018)

D. Neudecker, R. Capote, H. Leeb, Impact of model defect and experimental uncertainties on evaluated output. Nucl. Instrum. Methods Phys. Res. A **723**, 163 (2013)

N. Nishimura, T. Takiwaki, F.-K. Thielemann, The r-process nucleosynthesis in the various jet-like explosions of magnetorotational core-collapse supernovae. Astrophys. J. **810**, 109 (2015)

F. Nolden, K. Beckert, P. Beller, B. Franzke, C. Peschke, M. Steck, Experience and prospects of stochastic cooling of radioactive beams at GSI. Nucl. Instrum. Methods Phys. Res. Sect. A: Accel. Spectrom. Detect. Assoc. Equip. **532**, 329–334 (2004)

W.-J. Ong, A.A. Valverde, M. Brodeur, G. Bollen, M. Eibach, K. Gulyuz, A. Hamaker, C. Izzo, D. Puentes, M. Redshaw, R. Ringle, R. Sandler, S. Schwarz, C.S. Sumithrarachchi, J. Surbrook, A.C.C. Villari, I.T. Yandow, Mass measurement of $^{51}$Fe for the determination of the $^{51}$Fe$(p, \gamma)^{52}$Co reaction rate. Phys. Rev. C **98**, 065803 (2018)

R. Orford, N. Vassh, J.A. Clark, G.C. McLaughlin, M.R. Mumpower, G. Savard, R. Surman, A. Aprahamian, F. Buchinger, M.T. Burkey, D.A. Gorelov, T.Y. Hirsh, J.W. Klimes, G.E. Morgan, A. Nystrom, K.S. Sharma, Precision mass measurements of neutron-rich neodymium and samarium isotopes and their role in understanding rare-earth peak formation. Phys. Rev. Lett. **120**, 262702 (2018)

R. Orford, J.A. Clark, G. Savard, A. Aprahamian, F. Buchinger, M.T. Burkey, D.A. Gorelov, J.W. Klimes, G.E. Morgan, A. Nystrom, W.S. Porter, D. Ray, K.S. Sharma, Improving the measurement sensitivity of the Canadian penning trap mass spectrometer through PI-ICR. Nucl. Instrum. Methods Phys. Res. Sect. B: Beam Interact. Mater. Atoms **463**, 491–495 (2020)

A. Ozawa, T. Uesaka, M. Wakasugi, the Rare-RI Ring Collaboration, The rare-RI ring. Progress Theor. Exp. Phys. **2012**, 03C009 (2012)

A. Parikh, J. José, G. Sala, C. Iliadis, Nucleosynthesis in type I x-ray bursts. Progress Part. Nucl. Phys. **69**, 225–253 (2013)

D. Peña-Arteaga, S. Goriely, N. Chamel, Relativistic mean-field mass models. Eur. Phys. J. A **52**, 320 (2016)

J.M. Pearson, The quest for a microscopic nuclear mass formula. Hyp. Int. **132**, 59 (2001)

J.M. Pearson, N. Chamel, A.Y. Potekhin, A.F. Fantina, C. Ducoin, A.K. Dutta, S. Goriely, Unified equations of state for cold non-accreting neutron stars with brussels–montreal functionals – I. Role of symmetry energy. MNRAS **481**(3), 2994 (2018)

C. Pitrou, A. Coc, J.-P. Uzan, E. Vangioni, Precision big bang nucleosynthesis with improved helium-4 predictions. Phys. Rep. **754**, 1–66 (2018)

D. Puentes, G. Bollen, M. Brodeur, M. Eibach, K. Gulyuz, A. Hamaker, C. Izzo, S.M. Lenzi, M. MacCormick, M. Redshaw, R. Ringle, R. Sandler, S. Schwarz, P. Schury, N.A. Smirnova, J. Surbrook, A.A. Valverde, A.C.C. Villari, I.T. Yandow, High-precision mass measurements of the isomeric and ground states of $^{44}$V: improving constraints on the isobaric multiplet mass equation parameters of the $a = 44$, $0^+$ quintet. Phys. Rev. C **101**, 064309 (2020)

G. Racah, Sulla simmetria tra particelle e antiparticelle. Il Nuovo Cimento **14**, 322 (1937)

T. Radon, T. Kerscher, B. Schlitt, K. Beckert, T. Beha, F. Bosch, H. Eickhoff, B. Franzke, Y. Fujita, H. Geissel, M. Hausmann, H. Irnich, H.C. Jung, O. Klepper, H.-J. Kluge, C. Kozhuharov, G. Kraus, K.E.G. Löbner, G. Münzenberg, Y. Novikov, F. Nickel, F. Nolden, Z. Patyk, H. Reich, C. Scheidenberger, W. Schwab, M. Steck, K. Sümmerer, H. Wollnik, Schottky mass measurements of cooled proton-rich nuclei at the GSI experimental storage ring. Phys. Rev. Lett. **78**, 4701–4704 (1997)

M. Rayet, M. Arnould, M. Hashimoto et al., The p-process in Type II supernovae. Astron. Astrophys. **298**, 517 (1995)

M. Reichert, M. Obergaulinger, M. Eichler, M.Á. Aloy, A. Arcones, Nucleosynthesis in magneto-rotational supernovae. Mon. Not. R. Astron. Soc., MNRAS 501, 5733 (2021)

M.P. Reiter, S. Ayet San Andrés, S. Nikas, J. Lippuner, C. Andreoiu, C. Babcock, B.R. Barquest, J. Bollig, T. Brunner, T. Dickel, J. Dilling, I. Dillmann, E. Dunling, G. Gwinner, L. Graham, C. Hornung, R. Klawitter, B. Kootte, A.A. Kwiatkowski, Y. Lan, D. Lascar, K.G. Leach, E. Leistenschneider, G. Martínez-Pinedo, J.E. McKay, S.F. Paul, W.R. Plaß, L. Roberts, H. Schatz, C. Scheidenberger, A. Sieverding, R. Steinbrügge, R. Thompson, M.E. Wieser, C. Will, D. Welch, Mass measurements of neutron-rich gallium isotopes refine production of nuclei of the first $r$-process abundance peak in neutron-star merger calculations. Phys. Rev. C **101**, 025803 (2020)

K. Riisager, Halos and related structures **T152**, 014001 (2013)

R. Ringle, G. Bollen, P. Schury, S. Schwarz, T. Sun, Octupolar excitation of ion motion in a penning trap – a study performed at lebit. Int. J. Mass Spectrom. **262**, 33–44 (2007)

R. Ringle, G. Bollen, A. Prinke, J. Savory, P. Schury, S. Schwarz, T. Sun, The lebit 9.4t penning trap mass spectrometer. Nucl. Instrum. Methods Phys. Res. Sect. A: Accel. Spectrom. Detectors Assoc. Equip. **604**, 536–547 (2009)

L.M. Robledo, T.R. Rodríguez, R.R. Rodríguez-Guzmán, Mean field and beyond description of nuclear structure with the gogny force: a review. J. Phys. G: Nucl. Part. Phys. **46**, 013001 (2018)

X. Roca-Maza, X.V. Nas, M. Centelles, P. Ring, P. Schuck, Relativistic mean-field interaction with density-dependent meson-nucleon vertices based on microscopical calculations. Phys. Rev. C **84**, 054309 (2011)

M. Samyn, S. Goriely, P.-H. Heenen, J.M. Pearson, F. Tondeur, A hartree–fock–bogoliubov mass formula. Nucl. Phys. A **700**, 142 (2002)

G. Savard, R.C. Barber, C. Boudreau, F. Buchinger, J. Caggiano, J. Clark, J.E. Crawford, H. Fukutani, S. Gulick, J.C. Hardy, A. Heinz, J.K.P. Lee, R.B. Moore, K.S. Sharma, J. Schwartz, D. Seweryniak, G.D. Sprouse, J. Vaz, The Canadian penning trap spectrometer at Argonne, in *Atomic Physics at Accelerators: Mass Spectrometry* (Springer, Dordrecht, 2001), pp. 223–230

H. Schatz, A. Aprahamian, J. Görres, M. Wiescher, T. Rauscher, J.F. Rembges, F.-K. Thielemann, B. Pfeiffer, P. Möller, K.-L. Kratz, H. Herndl, B.A. Brown, H. Rebel, rp-process nucleosynthesis at extreme temperature and density conditions. Phys. Rep. **294**, 167–263 (1998)

B.E. Schultz, J.M. Kelly, C. Nicoloff, J. Long, S. Ryan, M. Brodeur, Construction and simulation of a multi-reflection time-of-flight mass spectrometer at the university of notre dame. Nucl. Instrum. Methods Phys. Res. Sect. B: Beam Interact. Mater. Atoms **376**, 251–255 (2016)

R.X. Schüssler, H. Bekker, M. BraÃŸ, H. Cakir, J.R. Crespo LÃ³pez-Urrutia, M. Door, P. Filianin, Z. Harman, M.W. Haverkort, W.J. Huang, P. Indelicato, C.H. Keitel, C.M. KÃ¶nig, K. Kromer, M. MÃ¼ller, Y.N. Novikov, A. Rischka, C. Schweiger, S. Sturm, S. Ulmer, S. Eliseev, K. Blaum, Detection of metastable electronic states by penning trap mass spectrometry. Nature **581**, 42–46 (2020)

P. Shuai, X. Xu, Y.H. Zhang, H.S. Xu, Y.A. Litvinov, M. Wang, X.L. Tu, K. Blaum, X.H. Zhou, Y.J. Yuan, X.L. Yan, X.C. Chen, R.J. Chen, C.Y. Fu, Z. Ge, W.J. Huang, Y.M. Xing, Q. Zeng, An improvement of isochronous mass spectrometry: velocity measurements using two time-of-flight detectors. Nucl. Instrum. Methods Phys. Res. Sect. B: Beam Interact. Mater. Atoms **376**, 311–315 (2016)

D.M. Siegel, J. Barnes, B.D. Metzger, Collapsars as a major source of r-process elements. Nature **569**, 241 (2019)

M. Smith, M. Brodeur, T. Brunner, S. Ettenauer, A. Lapierre, R. Ringle, V.L. Ryjkov, F. Ames, P. Bricault, G.W.F. Drake, P. Delheij, D. Lunney, F. Sarazin, J. Dilling, First penning-trap mass measurement of the exotic halo nucleus $^{11}$Li. Phys. Rev. Lett. **101**, 202501 (2008)

A. Sobiczewski, Y.A. Litvinov, M. Palczewski, Detailed illustration of the accuracy of currently used nuclear-mass models. Atomic Data Nucl. Data Tables **119**, 1–32 (2018)

J. Stadlmann, M. Hausmann, F. Attallah, K. Beckert, P. Beller, F. Bosch, H. Eickhoff, M. Falch, B. Franczak, B. Franzke, H. Geissel, T. Kerscher, O. Klepper, H.-J. Kluge, C. Kozhuharov, Y.A. Litvinov, K.E.G. Löbner, M. Matoš, G. Münzenberg, N. Nankov, F. Nolden, Y.N. Novikov, T. Ohtsubo, T. Radon, H. Schatz, C. Scheidenberger, M. Steck, H. Weick, H. Wollnik, Direct mass measurement of bare short-lived 44v, 48mn, 41ti and 45cr ions with isochronous mass spectrometry. Phys. Lett. B **586**, 27–33 (2004)

M. Steck, P. Beller, K. Beckert, B. Franzke, F. Nolden, Electron cooling experiments at the ESR. Nucl. Instrum. Methods Phys. Res. Sect. A: Accel. Spectrom. Detectors Assoc. Equip. **532**, 357–365 (2004)

M. Steck, Y.A. Litvinov, Heavy-ion storage rings and their use in precision experiments with highly charged ions. Progress Part. Nucl. Phys. **115**, 103811 (2020)

M.V. Stoitsov, J. Dobaczewski, W. Nazarewicz, S. Pittel, D.J. Dean, Systematic study of deformed nuclei at the drip lines and beyond. Phys. Rev. C **68**, 054312 (2003)

B. Sun, R. Knöbel, H. Geissel, Y.A. Litvinov, P.M. Walker, K. Blaum, F. Bosch, D. Boutin, C. Brandau, L. Chen, I.J. Cullen, A. Dolinskii, B. Fabian, M. Hausmann, C. Kozhuharov, J. Kurcewicz, S.A. Litvinov, Z. Liu, M. Mazzocco, J. Meng, F. Montes, G. Münzenberg, A. Musumarra, S. Nakajima, C. Nociforo, F. Nolden, T. Ohtsubo, A. Ozawa, Z. Patyk, W.R. Plaß, C. Scheidenberger, M. Steck, T. Suzuki, H. Weick, N. Winckler, M. Winkler, T. Yamaguchi, Direct measurement of the 4.6 mev isomer in stored bare 133sb ions. Phys. Lett. B **688**, 294–297 (2010)

I. Tanihata, H. Hamagaki, O. Hashimoto, Y. Shida, N. Yoshikawa, K. Sugimoto, O. Yamakawa, T. Kobayashi, N. Takahashi, Measurements of interaction cross sections and nuclear radii in the light $p$-shell region. Phys. Rev. Lett. **55**, 2676–2679 (1985)

M. Thoennessen, Reaching the limits of nuclear stability. Rep. Progress Phys. **67**, 1187–1232 (2004)

J.J. Thompson, Bakerian lecture: rays of positive electricity. Proc. R. Soc. Am. **89**, 1 (1913)

A. Tichai, R. Roth, T. Duguet, Many-body perturbation theories for finite nuclei. Front. Phys. **8**, 164 (2020)

C. Travaglio, T. Rauscher, A. Heger, M. Pignatari, C. West, Role of core-collapse supernovae in explaining solar system abundances of p nuclides. Astrophys. J. **854**, 18 (2018)

X.L. Tu, X.C. Chen, J.T. Zhang, P. Shuai, K. Yue, X. Xu, C.Y. Fu, Q. Zeng, X. Zhou, Y.M. Xing, J.X. Wu, R.S. Mao, L.J. Mao, K.H. Fang, Z.Y. Sun, M. Wang, J.C. Yang, Y.A. Litvinov, K. Blaum, Y.H. Zhang, Y.J. Yuan, X.W. Ma, X.H. Zhou, H.S. Xu, First application of combined isochronous and schottky mass spectrometry: half-lives of fully ionized $^{49}$Cr$^{24+}$ and $^{53}$Fe$^{26+}$ atoms. Phys. Rev. C **97**, 014321 (2018)

J. Uusitalo, J. Sarén, J. Partanen, J. Hilton, Mass analyzing recoil apparatus, mara. Acta Phys. Pol. B **50**, 319–327 (2019)

A.A. Valverde, M. Brodeur, G. Bollen, M. Eibach, K. Gulyuz, A. Hamaker, C. Izzo, W.-J. Ong, D. Puentes, M. Redshaw, R. Ringle, R. Sandler, S. Schwarz, C.S. Sumithrarachchi, J. Surbrook, A.C.C. Villari, I.T. Yandow, High-precision mass measurement of $^{56}$Cu and the redirection of the $rp$-process flow. Phys. Rev. Lett. **120**, 032701 (2018)

J. Van Schelt, D. Lascar, G. Savard, J.A. Clark, S. Caldwell, A. Chaudhuri, J. Fallis, J.P. Greene, A.F. Levand, G. Li, K.S. Sharma, M.G. Sternberg, T. Sun, B.J. Zabransky, Mass measurements near the $r$-process path using the canadian penning trap mass spectrometer. Phys. Rev. C **85**, 045805 (2012)

J. Van Schelt, D. Lascar, G. Savard, J.A. Clark, P.F. Bertone, S. Caldwell, A. Chaudhuri, A.F. Levand, G. Li, G.E. Morgan, R. Orford, R.E. Segel, K.S. Sharma, M.G. Sternberg, First results from the caribu facility: mass measurements on the $r$-process path. Phys. Rev. Lett. **111**, 061102 (2013)

D. Vautherin, D.M. Brink, Hartree-fock calculations with skyrme's interaction. I. Spherical nuclei. Phys. Rev. C **5**, 626 (1972)

M. Vilen, J.M. Kelly, A. Kankainen, M. Brodeur, A. Aprahamian, L. Canete, T. Eronen, A. Jokinen, T. Kuta, I.D. Moore, M.R. Mumpower, D.A. Nesterenko, H. Penttilä, I. Pohjalainen, W.S. Porter, S. Rinta-Antila, R. Surman, A. Voss, J. Äystö, Precision mass measurements on neutron-rich rare-earth isotopes at jyfltrap: reduced neutron pairing and implications for $r$-process calculations. Phys. Rev. Lett. **120**, 262701 (2018)

M. Vilen, J.M. Kelly, A. Kankainen, M. Brodeur, A. Aprahamian, L. Canete, R.P. de Groote, A. de Roubin, T. Eronen, A. Jokinen, I.D. Moore, M.R. Mumpower, D.A. Nesterenko, J. O'Brien, A.P. Perdomo, H. Penttilä, M. Reponen, S. Rinta-Antila, R. Surman, Exploring the mass surface near the rare-earth abundance peak via precision mass measurements at jyfltrap. Phys. Rev. C **101**, 034312 (2020)

H. von Groote, E.R. Hilf, K. Takahashi, A new semiempirical shell correction to the droplet model: gross theory of nuclear magics. At. Data Nucl. Data Tables **17**, 418 (1976)

C.F. von Weizsäcker, Zur theorie de kernmassen. Z. Phys. **96**, 431 (1935)

S. Wanajo, B. Müller, H.-T. Janka, A. Heger, Nucleosynthesis in the innermost ejecta of neutrino-driven supernova explosions in two dimensions. Astrophys. J. **853**, 40 (2018)

N. Wang, M. Liu, X.Z. Wu, Modification of nuclear mass formula by considering isospin effects. Phys. Rev. C **81**, 044322 (2010)

N. Wang, M. Liu, X. Wu, J. Meng, Surface diffuseness correction in global mass formula. Phys. Lett. B **734**, 215 (2014)

J.-Y. Wang, Y.-L. Tian, Y.-S. Wang, Z.-G. Gan, X.-H. Zhou, H.-S. Xu, W.-X. Huang, A multi-reflection time-of-flight mass analyzer at IMP/CAS. Nucl. Instrum. Methods Phys. Res. Sect. B: Beam Interact. Mater. Atoms **463**, 179–183 (2020)

M. Wang, W.J. Huang, F.G. Kondev, G. Audi, S. Naimi, The ame2020 atomic mass evaluation (II). Chin. Phys. C **45**, 030003 (2021)

R.N. Wolf, D. Beck, K. Blaum, C. Böhm, C. Borgmann, M. Breitenfeldt, N. Chamel, S. Goriely, F. Herfurth, M. Kowalska, S. Kreim, D. Lunney, V. Manea, E. Minaya Ramirez, S. Naimi, D. Neidherr, M. Rosenbusch, L. Schweikhard, J. Stanja, F. Wienholtz, K. Zuber, Plumbing neutron stars to new depths with the binding energy of the exotic nuclide $^{82}$Zn. Phys. Rev. Lett. **110**, 041101 (2013)

H. Wollnik, M. Przewloka, Time-of-flight mass spectrometers with multiply reflected ion trajectories. Int. J. Mass Spectrom. Ion Process. **96**, 267–274 (1990)

J.L. Wood, K. Heyde, W. Nazarewicz, M. Huyse, P. van Duppen, Coexistence in even-mass nuclei. Phys. Rep. **215**, 101–201 (1992)

J.W. Xia, W.L. Zhan, B.W. Wei, Y.J. Yuan, M.T. Song, W.Z. Zhang, X.D. Yang, P. Yuan, D.Q. Gao, H.W. Zhao, X.T. Yang, G.Q. Xiao, K.T. Man, J.R. Dang, X.H. Cai, Y.F. Wang, J.Y. Tang, W.M. Qiao, Y.N. Rao, Y. He, L.Z. Mao, Z.Z. Zhou, The heavy ion cooler-storage-ring project (hirfl-csr) at lanzhou. Nucl. Instrum. Methods Phys. Res. Sect. A: Accel. Spectrom. Detectors Assoc. Equip. **488**, 11–25 (2002)

J.W. Yoon, Y.-H. Park, S.J. Park, G.D. Kim, Y.K. Kim, Design of the multi-reflection time-of-flight mass spectrometer for the raon facility. EPJ Web Conf. **66**, 11042 (2014)

Z.Y. Zhang, Z.G. Gan, H.B. Yang, L. Ma, M.H. Huang, C.L. Yang, M.M. Zhang, Y.L. Tian, Y.S. Wang, M.D. Sun, H.Y. Lu, W.Q. Zhang, H.B. Zhou, X. Wang, C.G. Wu, L.M. Duan, W.X. Huang, Z. Liu, Z.Z. Ren, S.G. Zhou, X.H. Zhou, H.S. Xu, Y.S. Tsyganov, A.A. Voinov, A.N. Polyakov, New isotope $^{220}$Np: probing the robustness of the $n = 126$ shell closure in neptunium. Phys. Rev. Lett. **122**, 192503 (2019)